

1 **Geosystemics and Earthquakes**

2

3 Angelo De Santis <sup>(1,2)</sup>, Gianfranco Cianchini<sup>(1)</sup>, Rita Di Giovambattista<sup>(1)</sup>, Cristoforo Abbattista<sup>(3)</sup>,

4 Lucilla Alfonsi<sup>(1)</sup>, Leonardo Amoroso<sup>(3)</sup>, Marianna Carbone<sup>(3)</sup>, Claudio Cesaroni<sup>(1)</sup>, Giorgiana De

5 Franceschi<sup>(1)</sup>, Anna De Santis<sup>(1)</sup>, Alessandro Ippolito<sup>(1)</sup>, Dedalo Marchetti<sup>(1)</sup>, Luca Martino<sup>(2)</sup>,

6 Francisco Javier Pavón-Carrasco<sup>(1,4)</sup>, Loredana Perrone<sup>(1)</sup>, Alessandro Piscini<sup>(1)</sup>, Mario Luigi

7 Rainone <sup>(2)</sup>, Luca Spogli<sup>(1,5)</sup> and Francesca Santoro<sup>(3)</sup>

8

9

10 <sup>(1)</sup> Istituto Nazionale di Geofisica e Vulcanologia – Sez. Roma 2, Rome (Italy)

11 <sup>(2)</sup> Università G. D’Annunzio, INGEO Department, Chieti (Italy)

12 <sup>(3)</sup> Planetek Italia srl, via Massaua 12, Bari (Italy)

13 <sup>(4)</sup> Now at Facultad Física (UCM), Avd. Complutense, s/n. 28040 – Madrid (Spain)

14 <sup>(5)</sup> SpacEarth Technology, Rome, Italy

15

16

17 **Abstract**

18

19 Geosystemics [De Santis 2009, 2014] studies the Earth system as a whole focusing on the possible  
20 coupling among the Earth layers (the so called *geo-layers*), and using universal tools to integrate  
21 different methods that can be applied to multi-parameter data, often taken on different platforms. Its  
22 main objective is to understand the particular phenomenon of interest from a holistic point of view.

23 In this paper we will deal with earthquakes, considered as a long term chain of processes involving,  
24 not only the interaction between different components of the Earth’s interior, but also the coupling  
25 of the solid earth with the above neutral and ionized atmosphere, and finally culminating with the  
26 main rupture along the fault of concern [De Santis et al., 2015a]. Some case studies (particular  
27 emphasis is given to recent central Italy earthquakes) will be discussed in the frame of the  
28 geosystemic approach for better understanding the physics of the underlying complex dynamical  
29 system.

30

31

32

33

1 **1. Introduction**

2  
3  
4  
5  
6  
7  
8  
9  
10  
11  
12  
13  
14  
15  
16  
17  
18  
19  
20  
21  
22  
23  
24  
25  
26  
27  
28  
29  
30  
31  
32  
33  
34

The present times are difficult for humankind: although civilization, together with technology, has reached its greatest level, the cost to pay is that modernization has simultaneously involved some level of higher vulnerability than in the past (e.g. Nott, 2006). Humankind is affecting some parts of Nature, but, unfortunately, without perfect control. Natural hazards, e.g. hurricanes, earthquakes (EQs), floods, tsunamis, and other kinds of catastrophes, are often out of human control and the consequences are unpredictable. They happen as extreme events on the planet causing destruction and deaths (Meyers, 2009), and the occurrence of most of them looks as increasing dramatically in the last century (Peduzzi, 2005). Present society, although reaching a high technological level, is still very weak, and no strong remedy and rapid resilience are fully possible (Bunde et al., 2002).

There is no other solution than attempting to understand how our planet works and what possible future sceneries are. To do this, we cannot limit our approach to a reductionist one, but we also need to study the Earth as a whole system, where all parts are nonlinearly interconnected and useful for the system to evolve (e.g. Skinner and Porter, 1995). In contrast with the reductionist approach, the latter does not look at Earth as a precise clock system where all components have their distinct own purpose (often called as the Laplacian point of view), rather we have to consider it as an ensemble of cross-interacting parts put together in order to reach the same ambitious goal that, at the present knowledge, seems to be rare in the Universe: to maintain life (Lovelock, 1972). Earth system is both composed of living organisms and soft and hard engines, in a continuous balance and competition between life and death, heat and cold, complexity and simplicity, chaos and non-chaos.

In this paper we will remind the concepts of Geosystemics and then apply it to EQs, through some specific concepts such as the changes of Benioff strain, Entropy, temperature, etc., in the frame of a Lithosphere-Atmosphere-Ionosphere (LAI) coupling model, i.e. some quantities that are related to macroscopic features of the system under study.

Even if many efforts have been made towards a deeper knowledge of EQs, in terms of experimental, theoretical and numerical models (e.g. Aki & Richard, 2002; Bizzarri, 2011, 2012), their evolution phases are not exhaustively explained yet. A possible explanation of this uncertainty is the lack of knowledge regarding the source initiation, the fracture mechanisms and dynamics of the crust (e.g. Scholz, 2002). Moreover, each EQ initiates and develops in its proper geodynamical and

1 lithological settings, this giving an almost unique character to each event. Thus, to reach the  
2 knowledge necessary to recognise in advance the eventual rupture (failure) of the fault which causes  
3 the occurrence of the EQ is a greatly difficult task itself. Difficult as well is the possible explanation  
4 of the various and often weak phenomena affecting the above atmosphere and ionosphere, where  
5 even many external causes act to mix together signals which are different in spectral content and  
6 amplitudes.

7  
8 Despite all these difficulties, one of the most eminent seismologists, Hiroo Kanamori (1981),  
9 pointed out that some common physical mechanisms beneath the generation processes may act,  
10 although controlled by the local geodynamic forces and heterogeneities of the lithology (Baskoutas  
11 and Papadopoulos, 2014): this thought encourages the efforts towards a deeper knowledge of the  
12 physics behind such a complex phenomenon as the EQ.

13  
14 If the process of rupture that causes the EQ is still plenty of open issues and unanswered questions  
15 (e.g. Bizzarri, 2014), even more difficult is the understanding of the process of EQ preparation,  
16 although some efforts have been performed (e.g. Dobrovolsky et al. 1979, 1989; Sobolev et al.  
17 2002) as is thought to be accompanied by some exchanges of mass and energy, which can change  
18 the energy budget in the earth-atmosphere system over the seismogenic zone and, in fact, scientific  
19 literature reports a wide variety of phenomena preceding EQs which have been studied extensively  
20 with the aim of finding some recurrent and recognizable patterns: induced electric and magnetic  
21 fields, groundwater level changes, gas and infrared (IR) electromagnetic emissions, local  
22 temperature changes, surface deformations (see Cicerone et al., 2009 and De Santis et al., 2015a for  
23 more exhaustive reviews).

24  
25 Being Geosystemics introduced by one of the present coauthors, great part of this paper is based on  
26 own contributions from mostly already published material. However we attempted to give new  
27 insights on the idea of Geosystemics with also some unpublished own material or other researchers'  
28 contributions.

29  
30 At first, we place the present view of Geosystemics and show the application to some case studies.  
31 We also present a possible physical model that attempts to explain the found results. We then  
32 conclude with some feasible future directions and conclusions.

33  
34

1 **2. Geosystemics**

2  
3  
4 We depict here the general concepts of geosystemics in order to be then applied to EQs in the next  
5 section.

6  
7 Geosystemics looks at the Earth system in its whole: in particular, it focuses on self-regulation  
8 phenomena and relations among the parts composing the Earth. Dynamically speaking, it also  
9 searches for the possible trends of change or persistence of the specific system or sub-system under  
10 study (De Santis, 2009, 2014, De Santis and Qamili, 2015). To perform this, geosystemics applies  
11 mainly the concepts of entropy and information content to time series characterising the  
12 phenomenon under study: to measure and understand the physical world, not only energy and  
13 matter are important, but also information (Bekenstein, 2003). Interesting features of the complex  
14 system under study to investigate are: nonlinear coupling and new emergent behaviour, self-  
15 regulation, and irreversibility as important constituents of the Earth planet.

16  
17 The most important basic concept of geosystemics is that no layer of the Earth system is really  
18 isolate, rather it communicates (in terms of transfer of energy or particles) with the other ones. This  
19 concept is more strengthen in case of very powerful phenomena that release a large energy in a  
20 short time, such as the earthquakes in the lithosphere (for a M7 earthquake, around  $10^{15}$  Joule are  
21 released in some seconds), the lightning strikes in atmosphere (around  $10^9$  J in microseconds),  
22 etcetera. For instance, the information exchanged between contiguous parts of the Earth system  
23 producing increased entropy would allow us to better recognise and understand those irreversible  
24 processes occurring in the Earth's interior. As said in De Santis and Qamili (2015), "*Geosystemics*  
25 *has the objective to observe, study, represent and interpret those aspects of geophysics that*  
26 *determine the structural characteristics and dynamics of our planet and the complex interactions of*  
27 *the elements that compose it*" by means of some entropic measures.

28  
29 Together with this, the approach will be based on multi-scale/parameter/platform observations in  
30 order to better scrutinise the particular sub-systems of Earth under study as much as possible. This  
31 is a fundamental issue of geosystemics, because there is no better way to understand the behaviour  
32 of a complex system than looking at it from as many perspectives and points of view as possible.  
33 Recent advanced examples to observe the planet are from satellites (e.g. Chuvieco and Huete, 2009)  
34 and seafloors (Favali et al., 2015).

1 Geosystemics differs from the standard Earth System Science (e.g. Schneider and Boston, 1992;  
2 Skinner and Porter 1995; Jacobson et al., 2000; Butz, 2004): for instance, in the way it is applied by  
3 means of entropic measures to different physical quantities, this because entropy is the only entity  
4 that can be used to have some clues on the next future (please remind the second law of  
5 thermodynamics for which the entropy cannot decrease with time; e.g. Grandy, 2008).

6  
7 In this paper, we will concentrate the attention to the application to EQ physics study and the  
8 possibility for intermediate and/or short-term prediction. Here, with the term “prediction”, we mean  
9 the possibility to make a prediction about EQ occurrence, magnitude and location, with small  
10 uncertainty, i.e. in a deterministic way, in contrast with the probabilistic approach used in EQ  
11 forecast (please see also in the next section for other details on this question). In particular, we will  
12 explore the present state-of-the-art of the seismological diagnostic tools based on a macroscopic  
13 point of view. Particular emphasis will be dedicated to the above mentioned Shannon entropy. Later  
14 on, we also see another one that quantifies the sense of flow of information, the transfer entropy  
15 (Schreiber, 2000).

### 19 **3. Main seismological diagnostic tools**

20  
21  
22 The Holy Grail in seismology is to reach the capability of giving short-term prediction of large EQs  
23 thus eventually saving lives. Unfortunately, it is not an easy task as testified by the great all-out and  
24 full scale effort made with this aim in many fields of research (even far from the traditional field of  
25 seismology) and the corresponding huge amount of scientific papers claiming or denying success or  
26 simply attempting some important steps forward towards the goal. However, despite of the many  
27 attempts no significant success has been clearly counted (Hough, 2009).

28  
29 Regarding the methods to make EQ “predictions”, we can classify them in (mainly) *deterministic*  
30 and (mainly) *stochastic* methods. The bracket term “(mainly)” is placed because, actually, no  
31 method is only deterministic or stochastic. To be operative, we can define the latter methods as  
32 those that provide a forecast with some level of probability, for which the probability of no EQ is  
33 always different than zero, while the deterministic methods attempt to indicate the approaching of a

1 large EQ with some level of confidence, i.e. with small uncertainty in space and time of occurrence,  
2 and magnitude.

3  
4 Several statistical methods have been applied in the last decades to seismological data (mainly  
5 catalogs) with the aim of improving the knowledge on seismic phenomena. At present, the scientific  
6 community is involved in global projects to test and evaluate the performances of some well  
7 established algorithms in different tectonic environments (see <http://www.cseptestesting.org/>;  
8 <http://www.corssa.org/> websites). According to CSEP (Collaboratory for the Study of Earthquake  
9 Predictability), the most important steps of an earthquake prediction protocol are the following  
10 ones:

- 11
- 12 1. *Present a physical model that can explain the proposed precursor anomaly.*
- 13 2. *Exactly define the anomaly and describe how it can be observed.*
- 14 3. *Explain how a precursory information can be translated into a forecast and specify such a*  
15 *forecast in terms of probabilities for given space/time/magnitude windows.*
- 16 4. *Perform a test over some time that allows to evaluate the proposed precursor and its forecasting*  
17 *power.*
- 18 5. *Report on successful prediction, missed earthquakes, and false predictions.*

19 All above points are sequential, i.e. any mature precursor must sequentially satisfy those points.  
20 However, if a precursor is at an initial stage of maturity, for instance, it has been just discovered in  
21 some case studies, it can satisfy only some of the first points, lacking the following ones. An early  
22 stage of the work on some novel precursors cannot exclude the publication of initial investigations.  
23 This is the case of most recent found precursors (e.g. entropy) that we will present below.

24  
25  
26 In the present paper we surely meet the first two points, leaving the other three points to other  
27 papers where a deeper and extended study is performed on a few precursors (e.g. Piscini et al.  
28 2017).

29  
30 In this part, we will focus our attention to the deterministic methods, which are essentially based on  
31 a systematic catalog-based search of some peculiar *seismicity pattern recognition* in the given area  
32 of interest. A wide review on this topic is presented by Mignan (2008). In the following, we will  
33 describe *M8*, *RTP* (Reverse Tracing of Precursors), *PI* (Pattern Informatics) and *R-AMR* (Revised  
34 Accelerating Moment Release). The latter method is the most recent and is the one we know much

Codice campo modificato

Codice campo modificato

Formattato: Inglese (Stati Uniti)

Formattato: Giustificato, Interlinea: 1.5 righe

Formattato: Tipo di carattere:

Formattato: Inglese (Stati Uniti)

Formattato: Inglese (Stati Uniti)

Formattato: Inglese (Stati Uniti)

1 better, because some of the present co-authors have introduced the corresponding technique (De  
2 Santis et al., 2015b). For this reason, we will dedicate a specific section to it.

3  
4  
5  
6 *M8*

7  
8 *M8* was called in this way because it was designed by retroactive analysis of the seismicity  
9 preceding the greatest (*M8+*) EQs worldwide (e.g. Keilis-Borok and Kossobokov, 1990;  
10 Kossobokov, 2013). Some spatio-temporal functions are introduced in order to reconstruct a 7-  
11 dimensional phase space (the first three quantities are estimated for two values *C* of the average  
12 annual number of earthquakes in the sequence; usually *C*=10 and 20): *N*(*t*) is the number of main-  
13 shocks; *L*(*t*) the deviation of *N*(*t*) from the long-term trend; *Z*(*t*) the linear concentration of the main-  
14 shocks; and *B*(*t*) is the maximal number of aftershocks as a measure of EQ clustering (these  
15 functions are actually properly normalized). The algorithm then recognizes a well established  
16 criterion, defined by extreme values of the phase space coordinates, as a vicinity of the system  
17 singularity. When a trajectory enters the criterion, probability of extreme event increases to the level  
18 sufficient for its effective provision, so an alarm or a TIP, “Time of Increased Probability”, is  
19 declared. This algorithm can be ~~modified~~adapted for lower magnitudes and particular regions (e.g.  
20 CN8).

### 21 22 *The Reverse Tracing of Precursors (RTP)*

23  
24 The RTP is a method for medium-term (some months in advance) EQ prediction (Shebalin et al.,  
25 2006), which is based on a hierarchical ensemble of premonitory seismicity patterns. These patterns  
26 are: (1) “precursory chains” that are related with the correlation length (e.g. Zoller and Hainzl, 2002,  
27 Tyupkin and Di Giovambattista, 2005), (2) “intermediate-term patterns” that could be related to  
28 some accelerating seismicity (e.g. Gabrielov et al., 2000) and (3) “pattern recognition of infrequent  
29 events” that take into account several “opinions” to decide the validity of the calculated chain of  
30 events. If a sufficient number of “votes” is accumulated, then the chain is considered precursory  
31 (Shebalin et al., 2006). Some past EQs seem to have been predicted 6 to 7 months in advance,  
32 although a few false alarms also happened. Critical aspects are related to the predicted “area of  
33 alarm” that seems very large for a realistic application. ~~RTP has already evaluated by the gambling~~  
34 score, showing apparently only marginal or no significance in predicting earthquakes (Zechar and

**Formattato:** Tipo di carattere: Non Corsivo, Inglese (Stati Uniti)

**Formattato:** Inglese (Stati Uniti)

**Formattato:** Giustificato, Interlinea: 1.5 righe

**Formattato:** Tipo di carattere:

**Formattato:** Tipo di carattere: Inglese (Stati Uniti)

**Formattato:** Tipo di carattere: Colore carattere: Automatico

1 Zhuang 2010). However, Molchan (2011) criticised this conclusion, affirming that: “The statistical  
2 analysis of any prediction method with few target events and a short monitoring period is premature  
3 (this is the case of RTP)”.

#### 6 *Pattern Informatics (PI)*

8 The *PI* is a technique for quantifying the spatio-temporal seismicity rate changes in past seismicity (e.g. Rundle et al., 2002; Nanjo et al. 2005). Tiampo et al. (2006) derive a relationship  
9 between the “PI index” and stress change (e.g. Dieterich, 1994), based upon the crack propagation  
10 theory. In practice, the *PI* method measures the change in seismicity rate at each box of a pre-  
11 defined grid, relative to the background seismicity rate, through the division of the average rate by  
12 the spatial variance over all boxes. Then it identifies the characteristic patterns associated with the  
13 shifting of small EQs from one location to another through time prior to the occurrence of large  
14 EQs (Tiampo et al., 2006). Results are given in terms of mapping the “PI anomalies” which are  
15 located where a new large EQ can be expected. Holliday et al. (2007) have proposed a modification  
16 of *PI* by using complex eigenfactors, explaining the EQ stress field as obeying a wave-like equation.

#### 20 **4. Shannon Entropy and Shannon Information**

22 The Shannon Entropy  $h(t)$  (Shannon, 1948) is an important tool for the space-time characterization  
23 of a dynamical system. In general, for a system characterized by  $K$  possible independent states, this  
24 entropy is defined in a certain time  $t$  as follows:

$$25 \quad h(t) = -\sum_{i=1}^K p_i(t) \cdot \log p_i(t) \quad (1)$$

26 where  $p_i(t)$  is the probability of the system to be at the  $i$ -th state. For convenience, we impose  
27  $\sum_i p_i = 1$  and  $\log p_i = 0$  if  $p_i = 0$  to remove the corresponding singularity.

29 In literature, we can find a large number of physical interpretations of the Shannon Entropy. We  
30 consider here what we think it is the simplest one: it is a non-negative measure of our ignorance  
31 about the state of the system of concern. The Shannon Entropy has a great importance in evaluating  
32 and interpreting the behaviour of complex systems like Earth, in general, and EQs, in particular. On

**Formattato:** Tipo di carattere: Colore carattere: Automatico, Inglese (Stati Uniti)

**Formattato:** Tipo di carattere: Colore carattere: Automatico

**Formattato:** Tipo di carattere: Colore carattere: Automatico, Inglese (Stati Uniti)

**Formattato:** Tipo di carattere: Colore carattere: Automatico

**Formattato:** Tipo di carattere: Colore carattere: Automatico, Inglese (Stati Uniti)

**Formattato:** Inglese (Stati Uniti)

1 the other hand, we find in literature also the Shannon Information,  $I(t)$ , which is simply related to  
2  $h(t)$  as  $I(t) = -h(t)$ . Consequently, the Shannon information is a negative quantity that measures our  
3 knowledge on the state of the system when we know only the distribution of probability  $p(t)$  (Beck  
4 and Schlögl, 1993). Thus, this quantity measures our decreasing ability to predict the future  
5 evolution of the system under study.

6  
7

## 8 **5. Gutenberg-Richter law and $b$ -value**

9

10 The Gutenberg-Richter (GR) law has a central role in seismology (Gutenberg and Richter, 1944). It  
11 expresses the (decimal logarithm of the) cumulative number  $n$  of EQs with magnitude  $m$  equal to or  
12 larger than a magnitude  $M$ :

13

$$\log n(m \geq M) = a - bM \quad (2)$$

14

15 as a simple linear function of the magnitude  $M$ ;  $a$  and  $b$  are two constant parameters for a certain  
16 region and time interval, characterizing the associated seismicity; in particular,  $b$  is the negative  
17 slope of the above cumulative distribution and typically  $b \approx 1$ . Very soon it was recognized the  
18 importance of estimating the  $b$ -value as an indicator of the level of stress in a rock from laboratory  
19 experiments (Scholz, 1968), and only later the relationship has been confirmed for EQs  
20 (Schorlemmer et al., 2005).

21 Aki (1965) was the first to provide a simple expression to estimate  $b$  by means of the maximum  
22 likelihood criterion (with a correction proposed by Utsu, 1978):

$$b = \frac{\log e}{\bar{M} - M_{\min} + \Delta / 2} \quad (3)$$

23

24 with an uncertainty of  $\pm b / \sqrt{N}$ ;  $N$  is the total number of analyzed EQs;  $e = 2,71828 \dots$  is the Euler  
25 number, while  $\bar{M}$  is the mean value of the magnitudes of all considered EQs;  $M_{\min}$  is the minimum  
26 magnitude used in the  $b$ -value evaluation;  $\Delta$  is the resolution involved in the magnitude estimation,  
27 normally  $\Delta = 0.1$ . Usually the  $M_{\min}$  is the magnitude of completeness of a seismic catalog, i.e. the  
28 magnitude threshold at which or above the corresponding seismic catalog includes all occurred EQs  
29 in the region.

30

## 31 **6. Entropy and EQs**

32

1  
2  
3  
4  
5  
6  
7  
8  
9  
10  
11  
12  
13  
14  
15  
16  
17  
18  
19  
20  
21  
22  
23  
24  
25  
26  
27  
28

Now we apply the concept of Shannon Entropy to EQs. Most of this section is based on De Santis et al. (2011a) with some extension in order to clarify some concepts.

Given a sequence of EQs (in the form of a seismic catalog or a seismic sequence within a certain region) with non-negative (and normalized) probability  $P_i$  to have activated a certain  $i$ -th class of seismicity characterized by some range of magnitudes, the associated non-negative Shannon entropy  $h$  can be defined as (De Santis et al., 2011a):

$$h = -\sum_{i=1}^K P_i \cdot \log P_i \geq 0 \tag{4}$$

Since eq. (4) is applied to a discrete number of states,  $h$  is also called *discrete Shannon entropy*. It can be considered a reliable measure of uncertainty and missing information of the system under study.

Actually, the values of magnitude can assume a continuous range (in theory from  $M_{min}$  to infinity) then the discrete definition (4) becomes an integral definition (Shannon, 1948; Ihara, 1993):

$$H = -\int_{M_{min}}^{\infty} p(M) \cdot \log p(M) dM \tag{4a}$$

where  $H$  is now called *continuous (or differential) Shannon entropy* to be distinguished from  $h$ , and  $p(M)$  is the probability density function (*pdf*) of the magnitudes  $M$ , such as

$$p(M) = \frac{d}{dm} \sum_{i,m \leq M} P_i(m),$$

and

$$\int_{M_{min}}^{\infty} p(M) dM = 1$$

It is worth noticing that moving from the discrete definition (4) to the continuous (4a), the property of non-negative  $h$  is lost by  $H$ , that can assume also negative values (e.g., Ihara, 1993). This is not evident from the work by De Santis et al. (2011a), so we will spend here some words about it.

The two definitions of the Shannon entropy are related by the following equation:

$$H = h + \log \Delta \tag{5}$$

1 where  $\Delta$  is the sampling step of the continuous *pdf* in order to let it discrete in  $h$  (e.g. Klir 2006). It  
2 is evident from (5) that when  $\Delta$  tends to zero,  $H$  will diverge to  $-\infty$ . Thus, the continuous entropy  $H$   
3 is not a limit for  $\Delta \rightarrow 0$  of the Shannon discrete entropy  $h$  and, consequently, it is not a measure of  
4 uncertainty and information. However, the continuous Shannon entropy can be used to measure  
5 differences in information (Ihara 1993).

6  
7 However, when the classes of magnitude are loose, e.g. for  $\Delta \approx 1$  we will have  $H \approx h$ : De Santis et al.  
8 (2011a) considered  $\Delta = 0.5$  so the difference between discrete and continuous entropies was only 0.3.

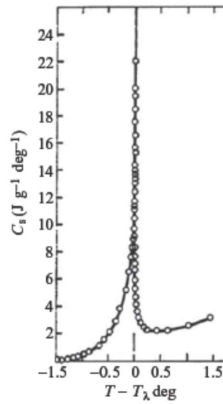
9  
10 De Santis et al. (2011a) have shown that if the  $p(M)$  is the GR probability distribution, then  $H$  can  
11 be expressed in terms of the  $b$ -value:

$$H \approx 0.072 \cdot \log b \quad (6)$$

12  
13  
14  
15 This relation is detailed and proved in the Appendix. The above expression provides an alternative  
16 explanation of the typical decrease of b-value as seismic precursor (e.g. Suga et al. 2014 for the  
17 case of 6 April 2009 M6.3 L'Aquila earthquake in Central Italy) as an increase of entropy  
18 culminating almost at the mainshock (De Santis et al. 2011a).

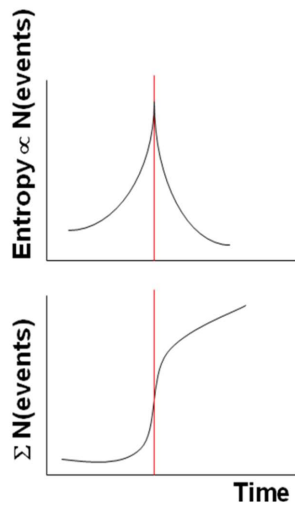
## 19 20 **7. Entropy and critical point theory**

21  
22 An *ergodic* dissipative system can have a critical point where the system undergoes through a  
23 transition. The ergodic property means that the system averages in real 3D space are equivalent to  
24 averages in the ideal reconstructed phase space (e.g. Takens, 1981, De Santis et al., 2011b). As an  
25 example, Fig. 1 reports the behaviour of the *specific heat* around a critical point occurring at  
26 temperature  $T_\lambda$  degree. It is interesting how the system approaches the critical temperature as a  
27 power law. In addition, if the system changes its temperature linearly in time, the same plot is  
28 expected versus time.



1  
2 **Fig. 1.** Specific heat of  $^4\text{He}$  as a function of  $T - T_\lambda$  in Kelvin.  $T_\lambda$  is the temperature at which the critical system has a  
3 transition (critical point) (Adapted from Stanley, 1971).

4  
5 More generally, if we replace the increasing temperature with the system entropy, then the system  
6 reaches its critical point (vertical red line in Fig.2) at the largest Entropy and approaches it with an  
7 accelerating power law in its cumulative of *punctuated* events (we intend here for an “event” as an  
8 anomalous behaviour of the system evolution, e.g. when its signal level is larger than a certain  
9 number of standard deviation,  $\sigma$ , e.g.  $2.5 \sigma$ ).



10  
11 **Fig. 2.** Idealized Shannon entropy (above diagram) and cumulative number of events (bottom diagram) for a dissipative  
12 system around its critical point, indicated by the vertical red line.

1  
 2 After the critical point, the curve behaves as a decelerating power law. Fig. 2 depicts both the  
 3 idealized behaviours for the entropy and the cumulative number of events.  
 4 We will see in the following how these patterns are reproduced in the case studies of some Italian  
 5 seismic sequences.

6  
 7 **8. Entropy studies of two Italian seismic sequences**  
 8  
 9

10 In this part, we show two case studies in Italy: the 2009 L'Aquila and the 2012 Emilia seismic  
 11 sequences, both producing a main-shock of around M6 (precisely local and moment magnitudes,  
 12 ML5.9 and Mw6.2 for L'Aquila and local magnitude ML5.9 for Emilia). Main characteristics of the  
 13 two seismic sequences are given in Table 1. The first case was already analysed and discussed by  
 14 De Santis et al. (2011a). However, we will make here some alternative/complementary analyses,  
 15 with respect to those already published. The second case study is original and never published so far.  
 16 In both cases we considered all earthquakes with a minimum magnitude equal to (entropy analysis)  
 17 or well above (R-AMR; see section 9) the completeness magnitude of the earthquake catalogs, that  
 18 was found of M1.4+ and M2+ for L'Aquila and Emilia earthquake sequences, respectively.  
 19  
 20

Sequence ID	Main-shock Parameters						# data (foreshocks)	R <sub>max</sub> (km)	M <sub>min</sub> (*)
	Coord. (lat, lon) in degree	Depth (km)	Date	t <sub>f</sub> in days from 1 May 2005 (predicted)	Fault style	Magnitude (predicted) *			
L'Aquila	42.34N 13.38E	8.3	6 Apr 2009	1436.06 (1437.4)	N	5.9 (5.3±0.5)	17	300	4.0
Emilia	44.89N 11.23E	6.3	20 May	2576.09 (2577.7)	R	5.9 (5.7±0.5)	38	300	4.0

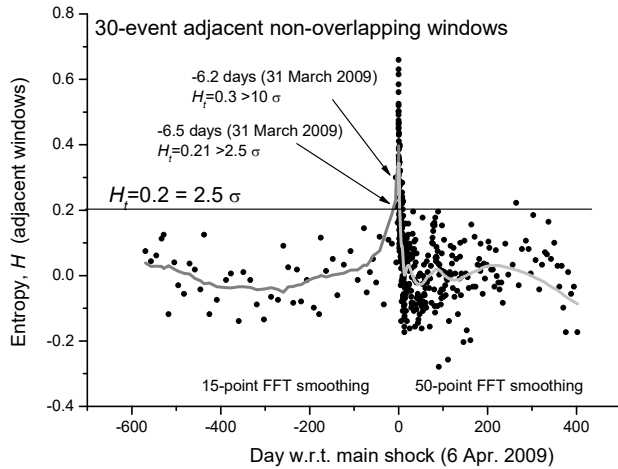
			2012						
--	--	--	------	--	--	--	--	--	--

\* normally deduced from eq. (2a or 2b)

1 **Table 1** - Main data related to the two Italian seismic sequences under study: (from left to right) the label, the main-  
2 shock source parameters, the number of data points (foreshocks) used in the fitting stage; the maximum distance from  
3 the main-shock epicentre defining the selection area and the minimum threshold magnitude of the selected events there  
4 considered. We provide also a rough estimation of the predicted magnitude (within brackets) of the impending main-  
5 shock (see text). N and R in the Fault style column stand for Normal, and Reverse focal mechanism, respectively. Rmax  
6 and Mmin are the largest area and minimum magnitude, respectively, considered in the analyses of R-AMR, while for  
7 the entropy analyses we considered always the completeness magnitude (M1.4 and M2 for L'Aquila and Emilia  
8 Earthquakes).

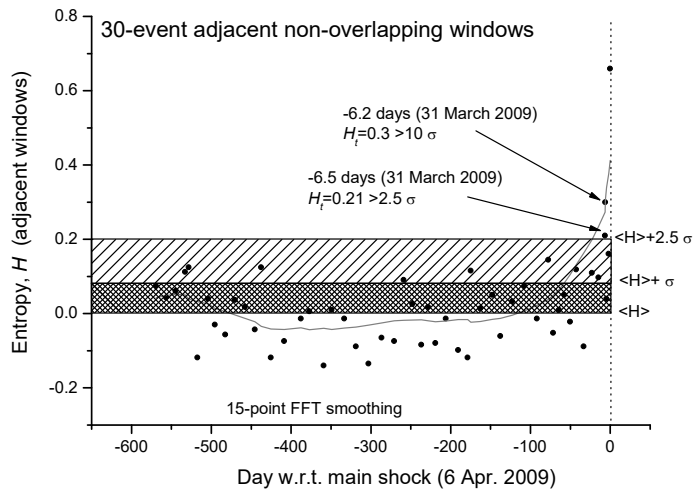
9  
10 *The 2009 L'Aquila seismic sequence*

11  
12 As mentioned in De Santis et al. (2011a), Shannon entropy can be estimated in three different ways:  
13 cumulative, moving overlapping or distinctively temporal windows. For the first case study, i.e. the  
14 2009 L'Aquila (Central Italy) seismic sequence, we will consider adjacent non-overlapping moving  
15 windows. In Fig.3 we show the estimation of the Shannon Entropy based on non-overlapping  
16 windows of 30 M1.4+ seismic events occurred in a circular area of 80 km around the main-shock  
17 epicentre. The low number of events used for the analysis in each window was chosen to better  
18 follow even shorter fluctuations of entropy, especially for the foreshocks. It is interesting that two  
19 distinct entropy values before the main-shock occurrence are larger than the threshold  $H_t=2.5 \sigma$  (the  
20 mean value of entropy,  $\langle H \rangle$ , is practically zero). To better visualize the mean behaviour of entropy,  
21 the gray curve defines a reasonable smoothing of the entropy values: 15-point FFT before the main-  
22 shock and 50-point FFT smoothing after the main-shock. The different kind of smoothing is related  
23 to the different rate of seismicity before and after the main-shock. It is interesting to notice that the  
24 smoothed gray curve of the Shannon Entropy reproduces the expected behavior of a critical system  
25 around its critical point (as shown in Fig.1, but with time as x-axis ), with the main-shock as critical  
26 point.  
27



1  
 2 **Fig. 3.** Shannon entropy for L'Aquila seismic sequence from around 1.5 year before the main-shock to around 1 year  
 3 after, calculated for a circular area of 80 km around the main-shock epicenter. Each point is the entropy analysis based  
 4 on non-overlapping windows, each composed by 30 foreshocks. The gray curve defines a reasonable smoothing of the  
 5 entropy values: 15-point FFT before the main-shock and 50-point FFT smoothing after the main-shock. The different  
 6 kind of smoothing is related to the different rate of seismicity before and after the main-shock. It is interesting how the  
 7 smoothed curve reproduces the expected behavior of a critical system around its critical point. (Adapted from Wu et al.  
 8 2016).

9  
 10 We can even analyse in more detail the same curve, but expanded in the period before the main-  
 11 shock (Fig. 4). We confirm that, around 6 days before the main-shock, there is the persistence of  
 12 two consecutive values of entropy greater than  $2.5\sigma$  (the larger value is even greater than  $10\sigma$ ). An  
 13 interesting question to better investigate in more case studies will be: could this persistence of larger  
 14 values of entropy be considered a reliable precursor of the imminent main-shock?  
 15



1  
 2 **Fig. 4.** Detail of the Shannon entropy for L'Aquila seismic sequence from around 1.5 year before the main-shock to the  
 3 main-shock occurrence. Each point is the entropy analysis based of non-overlapping windows, each composed by 30  
 4 foreshocks. The mean value of the entropy,  $\langle H \rangle$ , which is almost zero, and one and two standard deviations are also  
 5 shown. The gray curve defines a reasonable smoothing of the entropy values with 15-point FFT.

6  
 7 *The 2012 Emilia seismic sequence*

8  
 9 In this specific case study, we will consider moving and partially overlapping windows, each  
 10 composed of around 200 seismic events and overlapping of 20 events. This kind of analysis allows  
 11 us to have directly a smoother curve of entropy, without resorting to a subsequent smoothing  
 12 operation as done instead in the previous case.

13  
 14 In Fig. 5 we plot the Shannon entropy for Emilia seismic sequence from 2000 to 2014, as estimated  
 15 over all M2+ EQs occurred around 150 km the first major EQ. The significant increase starting  
 16 around 2010 is probably real and related to the preparation phase of the two major EQs occurred on  
 17 20 and 29 May, 2012 with local magnitudes 5.9 and 5.8, respectively, where the entropy reaches the  
 18 maximum value (in this case around 0.3). The gray area defines the estimated error in computing  
 19 the entropy.

20

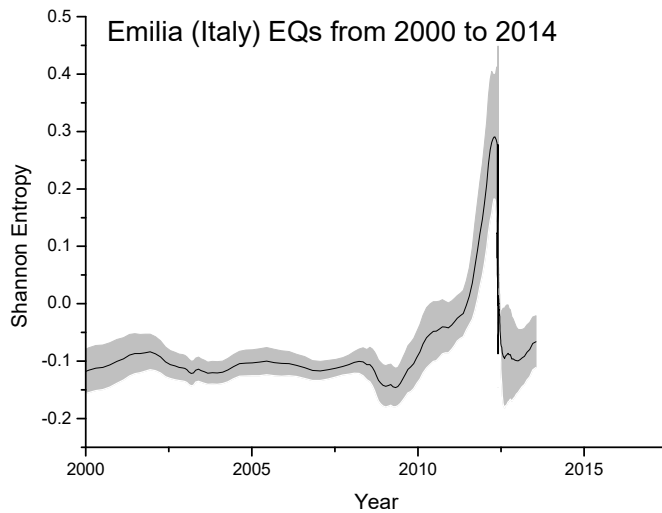


Fig. 5. Shannon entropy for Emilia seismic sequence from 2000 to 2014. The significant increase from around 2010, with the maximum at around the main-shock occurrence, is expected to be real. The gray area defines the statistically estimated (1 standard deviation) error in computing the entropy.

As a general remark of this section, it is true that we applied the entropy analysis to only two case studies, but in most occasions, we could extend the results found analyzing *b*-value to the entropy, via the equation (6). The introduction of the Shannon entropy in the analysis of a seismic sequence provides a more physical and statistical meaning to the potential precursory decrease of the *b*-value in terms of an increasing of entropy of the underlying physical system.

### 9. Accelerated Moment Release revisited: the case of L'Aquila and Emilia EQs

Benioff (1949) proposed a simple way to estimate the strain-rebound increment,  $\varepsilon_i$ :

$$s_i = \sqrt{E_i} = k_i \cdot \varepsilon_i \quad (7)$$

where  $E_i$  is the energy released by the EQ, i.e.  $10^{\alpha M + \beta}$  ( $\alpha=1.5$ ,  $\beta=4.8$  for energy expressed in Joule, although Benioff used slightly different values), and  $k_i = (\mu P V_i / 2)^{0.5}$  ( $\mu$ =shear or rigidity modulus,  $V_i$ = volume of the *i*-th fault rocks,  $P$  is the fraction of energy transmitted in terms of seismic waves; usually it is considered  $P \approx 1$ ). This theory is based on Reid (1910) arguments of the elastic rebound.

To take account of the cumulative effect of a series of  $N$  EQs at the time  $t$  of the last  $N$ -th EQ, Benioff introduced therefore what is now called *cumulative Benioff strain*  $s$ :

- Formattato: Colore carattere: Automatico
- Formattato: Colore carattere: Automatico, Inglese (Stati Uniti)
- Formattato: Colore carattere: Automatico
- Formattato: Colore carattere: Automatico, Inglese (Stati Uniti)
- Formattato: Colore carattere: Automatico
- Formattato: Colore carattere: Automatico, Inglese (Stati Uniti)
- Formattato: Colore carattere: Automatico
- Formattato: Colore carattere: Automatico, Inglese (Stati Uniti)

$$s(t) = \sum_{i=1}^{N(t)} s_i = \sum_{i=1}^{N(t)} \sqrt{E_i} = 10^{\beta} \sum_{i=1}^{N(t)} 10^{0.75M_i} \quad (8)$$

with  $\beta' = \beta/2 = 2.4$ . It is important to notice that, according to Benioff (1949), the cumulative strain (8) is that accumulated *on the fault* under study.

Extending the meaning of (8) to the strain accumulated over a larger area around the epicentre, Bufe and Varnes (1993) obtained interesting results with the so-called *Accelerating Moment Release (AMR)* approach that consists in fitting the cumulative value  $s(t)$  expressed as in (8), with a power law in the time to failure  $t_f$ , i.e. the theoretic time of occurrence of the main shock:  $s(t) = A + B(t_f - t)^m$ , where  $A$ ,  $B$  and  $m$  are appropriate empirical constants ( $m$  is expected between 0 and 1: typical value is 0.3; Mignan, 2008). The fitting process gives as an outcome the time  $t_f$  together with the expected magnitude, which is related to either  $A$  or  $B$ :

$$M_p(A) = \frac{\log(\Delta s_{last}) - \beta'}{0.75} \quad (9a)$$

where  $\Delta s_{last} = A - s_{last}$  and  $s_{last}$  is the cumulative Benioff strain at the last precursory event considered (namely the  $N$ -th EQ). In this expression one speculates that the main-shock will be the next EQ striking after the  $N$ -th, but the occurrence of many smaller EQs after the last analysed shock and before the predicted time  $t_f$  cannot be excluded.

An alternative formulation, based on the parameter  $B$ , has been given by Brehm & Braile (1999):

$$M_p(B) = \frac{\log|B| - \beta' - 0.14}{0.738} \quad (9b)$$

A criticism to this method came from Hardebeck et al. (2008) who pointed out the arbitrariness in the critical choice of the temporal and spatial criteria for data selection, i.e. the initial precursory event of the *AMR* curve and the extension of the inspected region.

To circumvent this criticism, De Santis et al. (2015) introduced what they called R-AMR, i.e. the Revised Accelerating Moment Release (R-AMR), as a better way of applying the AMR by weighting the EQs magnitudes in a certain area, according to an appropriate attenuation function  $G = G(R)$ , where  $R$  is the distance of a given EQ epicentre with respect to the *impending slipping fault*. In particular, the Benioff Strain produced at the fault level is expressed by a reduced Benioff strain  $\hat{s}(t) = s \cdot G$  called “reduced” because the action of the function  $G$ , which is normally less than unity (i.e.  $G \leq 1$ ), is to lower the value of the typical Benioff strain, normally according to the distance  $R$  from the centre of the region of study. As area of interest, a circle is taken with the

Codice campo modificato

1 corresponding Dobrovolsky radius,  $r(\text{km})=10^{0.43M}$  with  $M=EQ$  magnitude (Dobrovolsky et al.,  
2 1979).

3  
4 Thus, the expression for the cumulative *reduced* strain becomes:

5  
6 
$$\tilde{s}(t) = \sum_{i=1}^{N(t)} \tilde{s}_i = \sum_{i=1}^{N(t)} \sqrt{E_i} \cdot G(R_i) = 10^{\beta'} \sum_{i=1}^{N(t)} 10^{0.75M_i} G(R_i) \quad (8b)$$

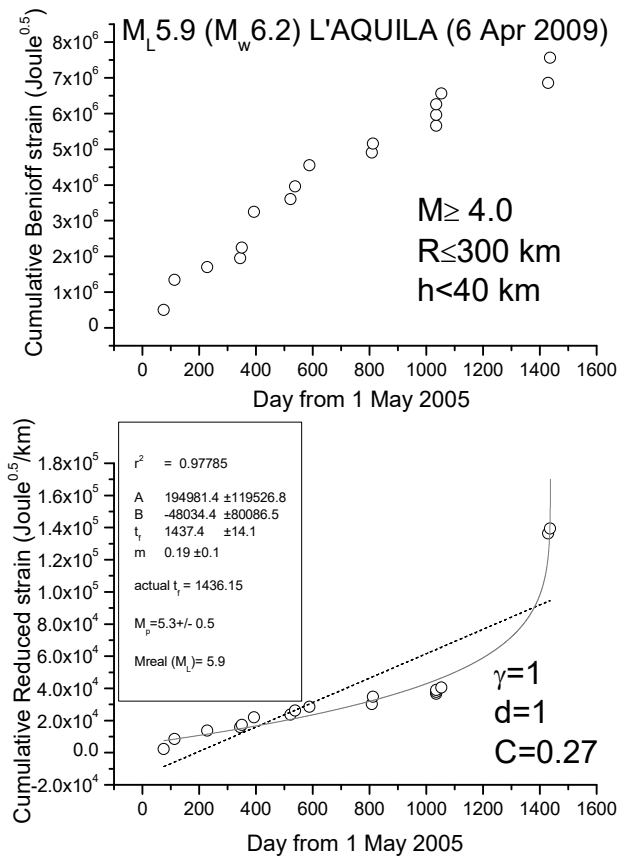
7  
8 De Santis et al. (2015b) applied with success their revisited method to the three most important  
9 seismic sequences occurred in Italy in the last ten years. In addition, they also showed that, for a  
10 particular seismic swarm (i.e. with no mainshock), R-AMR performs better than AMR, not  
11 providing a false alarm.

12  
13 *R-AMR for the 2009 L'Aquila and 2012 Emilia seismic sequences*

14  
15 We show here two case studies, L'Aquila and Emilia seismic sequences, where the application of  
16 R-AMR is made much simpler than the one firstly proposed in De Santis et al. (2015b). Although  
17 that way of applying of R-AMR is more rigorous because all EQs above the minimum magnitude of  
18 completeness are considered, we show here that a simpler application is possible, where considering  
19 a very simple attenuation function of the form  $G(R_i)=d/R_i^\gamma$ , with  $d$  (normally 1km),  $R_i$  in km and  
20 with  $\gamma \approx 1$ , at the cost of considering a larger minimum magnitude threshold of around  $M4$ . Figs 6a  
21 and 6b show the results for the cases of L'Aquila and Emilia sequences, where we apply to all  
22 shallow (depth  $h \leq 40$  and  $h \leq 80$  km, respectively)  $M4+$  EQs both AMR and R-AMR analyses (top  
23 and bottom of each figure, respectively). Then, we then consider a 300 km size for the regions  
24 where we applied R-AMR analysis. This size is comparable with the corresponding Dobrovolsky's  
25 radius. Both the analyses stop well before the main-shocks that are not so considered in the  
26 calculations. We notice that the time of preparation is rather long for both sequences, i.e. practically  
27 starting at the beginning of the whole period of investigation (May 2005). This fact could be simply  
28 interpreted as the larger foreshocks anticipate the beginning of the seismic acceleration with respect  
29 to the smaller ones, which were the most in the previous analyses in De Santis et al. (2015b).

30 The goodness of the power law fit with respect to the linear regression can be quantified by the C-  
31 factor which is the square root of the ratio between the RMS of the power law and the RMS of the  
32 best linear fit (Bowman et al., 1998): the lower the C-factor than 1, the better the power law fit is  
33 with respect to the line.

1  
2  
3

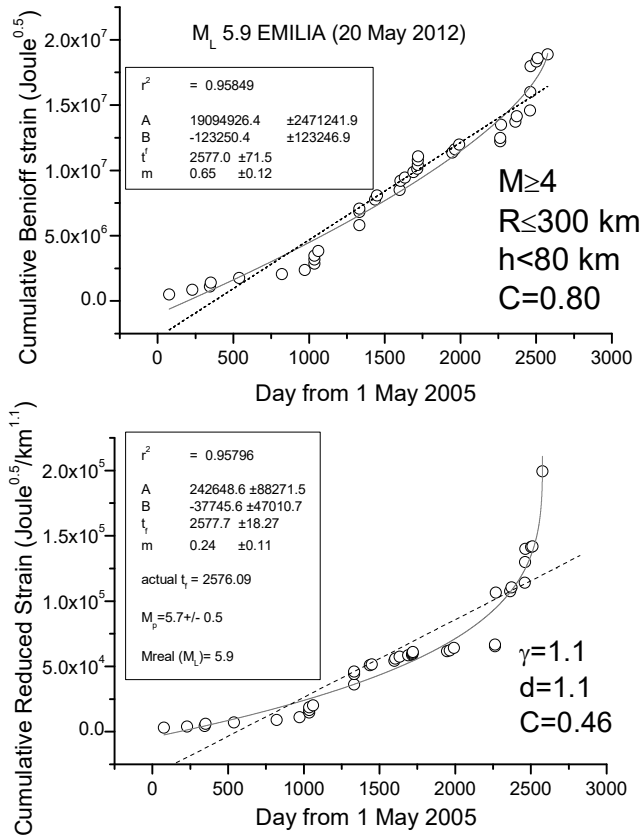


4  
5  
6  
7  
8  
9

**Figure 6a** — Analyses of L'Aquila seismic sequence  $M \geq 4$  EQs (main-shock not shown and not used in the analysis): top) ordinary AMR method; bottom) R-AMR method. Dashed line represents the best linear fit, while solid gray curve is the best power law fit. Results of the fit are shown in the frame inside the graph at the bottom;  $r^2$  is the coefficient of determination, providing a measure of the quality of the fit (the closer to 1, the better the fit).

10 We find a clear seismic acceleration for both seismic sequences, quantified by a low value of C  
11 (0.27 for L'Aquila sequence and 0.46 for Emilia sequence) and a great determination coefficient  
12 ( $r^2 > 0.95$  in both cases). In addition, the predicted magnitudes are comparable with (although lower

- 1 than) the real ones. In both cases, the beginning of clear acceleration starts around 1.5 year before
- 2 the main-shock.



3  
 4 **Figure 6b** — Analyses of Emilia seismic sequence  $M \geq 4$  EQs (main-shock not shown and not used in the analysis): top)  
 5 ordinary AMR method; bottom) R-AMR method. Here the ordinary ASR also showed a little acceleration ( $C$ -  
 6 factor=0.80) but the R-AMR version is much better ( $C$ -factor=0.46). Dashed line represents the best linear fit, while  
 7 solid gray curve is the best power law fit. Results of the fit are shown in the frames inside the graphs;  $r^2$  is the  
 8 coefficient of determination, providing a measure of the quality of the fit (the closer to 1, the better the fit).

9  
 10 The above cases represent two of the four seismic sequences happened in Italy in the last 15 years.  
 11 Another seismic sequence occurred in south Italy in 2010 and culminated with a M5 in Pollino area  
 12 showing an analogous acceleration before the mainshock (De Santis et al., 2015). Only the most  
 13 recent seismic sequence of the Amatrice-Norcia (Central Italy) earthquakes in 2017, did not have  
 14 neither acceleration nor foreshocks before the first major earthquake (24 August 2016 M6 Amatrice

1 earthquake). Therefore, the two case studies here shown are very representative of the most recent  
2 seismicity in Italy that has expressed in terms of a series of earthquakes culminating with a  
3 mainshock.

#### 5 **10. Lithosphere-Atmosphere-Ionosphere Coupling (LAIC)**

6  
7 Geosystemics sees the planet in its entirety, where all geo-layers “communicate” each other, in  
8 terms of exchange of matter and/or energy, i.e. what Bekenstein (2003) called with the more generic  
9 term of “information”. An important recent model is the so-called Lithosphere-Atmosphere-  
10 Ionosphere Coupling (LAIC) for which before a large EQ, in its preparation phase, some precursory  
11 anomalies can appear in atmosphere and/or in ionosphere (e.g. Pulinets and Boyarchuk, 2004).

12  
13 The state of the ionosphere is particularly sensitive to the LAIC. Its presence as ionised layer at 50-  
14 1000 km altitude above the Earth’s surface is important to detect any electromagnetic change in the  
15 circumterrestrial environment (Kelley, 2009). Comprehensive reviews of the papers describing the  
16 measurements of the seismo-ionospheric signals are reported in De Santis et al. (2015b) and Jin et  
17 al. (2015). In addition, Pulinets and Davidenko (2014) make a discussion on the temporal and  
18 spatial variability of the ionospheric precursor summarizing the results obtained by a large number  
19 of authors so far. In particular, they describe in detail which is the role of the Global Electric Circuit  
20 in transferring information from the Earth’s surface up to the ionosphere.

21  
22 The finding of atmospheric anomalies prior to large EQs is more recent and also debated as well.

23  
24 In this section, we remind some of those phenomena, the nature and characteristics of which are  
25 more directly of interest for the understanding of LAIC.

#### 27 *Pre-EQ ionospheric evidences from ground-based observations*

28  
29 A coupling (post-seismic) effect of an EQ to the above atmosphere is already well known: it can  
30 appear just after the occurrence of a sufficiently large event, and it is related to the possibility of  
31 observing the effect of the propagation of acoustic gravity waves in the ionosphere (e.g. Row, 1967).  
32 Recently, this effect has been clearly detected as wave-like fluctuations of the Total Electron  
33 Content (TEC) in ionosphere 21 minutes after the April 25, 2015 M7.8 Nepal EQ

Formattato: Francese (Francia)

Codice campo modificato

1 (<http://gpsworld.com/gps-data-show-how-nepal-quake-disturbed-earths-upper-atmosphere/>; last  
2 access on 23 October 2017).

3  
4 Important precursory effects of LAIC before large EQs can be detected in the ionosphere from  
5 ground-based observational systems like ionosondes and GPS (Global Positioning System)/GNSS  
6 (Global Navigation Satellite System) receivers.

7  
8 A large number of papers report some variations of ionospheric parameters before many large EQs,  
9 such as the F2-layer critical frequency (foF2) (Hobara and Parrot, 2005; Liu et al., 2006; Dabas et  
10 al., 2007; Perrone et al. 2010; Xu et al. 2015) and the sporadic E layer (Es) (Silina et al. 2001;  
11 Ondoh 2003; Ondoh and Hayakawa 2006).

12  
13 The study of foF2 alone is a very “inconvenient” ionospheric parameter for the role of EQ precursor,  
14 because, besides the geomagnetic activity effects, there would be many other reasons for non-EQ  
15 related foF2 variations. Therefore, a multi-parameter analysis is preferable and some works have  
16 analysed more ionospheric parameters at the same time, in order to achieve a more robust result.  
17 For instance, in the periods of time preceding all crustal EQs in Central Italy with magnitudes  $M >$   
18 5.0 and the epicenter depth  $< 50$  km, Perrone et al. (2010) have considered the ionospheric sporadic  
19 E layer (Es) together with the blanketing frequency of Es layer (fbEs) and foF2, by analysing data  
20 from the ionospheric observatory inside the preparation zone. According to these authors, the found  
21 deviations of ionospheric parameters from the background level can be related to the magnitude and  
22 the epicentre distance of the corresponding EQ.

23  
24 There is significant literature related to the analysis of the ionospheric effects before and during an  
25 EQ revealed by GPS/GNSS ground-based measurements, in terms of TEC fluctuations and  
26 scintillation anomalies that have been claimed to be detected some days before the EQs. Just to  
27 mention the more recent works, Mancini et al. (2014) analysed 5 years of GNSS-based ionospheric  
28 TEC data to produce maps over an area surrounding the epicentre of the 2009 L’Aquila EQ. An  
29 interesting ionospheric anomaly was found in the night of 16 March 2009, anticipating the main  
30 shock by 3 weeks and could be connected with it. Contadakis et al. (2014) reported on the analysis  
31 of the total electron content (TEC) from eight GPS stations of the EUREF network by using  
32 discrete Fourier to investigate the TEC variations over the Mediterranean region before and during  
33 the 12 October 2013 Crete, Greece EQ. Over an area of several hundred kilometers from the EQ  
34 epicentre, all stations used in this study observed an increase of 2-6 TECU from 10 October to 15

1 October 2013, likely related to the EQ. Akhondzadeh (2015) applies a complex algorithm, the  
2 Firefly Algorithm (FA), as a robust predictor to detect the TEC seismo-ionospheric anomalies  
3 around the time of the some powerful EQs (27 February 2010 M8.8 Chile, 11 August 2012 M6.4  
4 Varzeghan and 16 April 2013 M7.7 Saravan). Significant anomalies were observed 3 - 8 days  
5 before the EQs.

6 A recent paper by Kuo et al. (2015) presents the application of the LAIC model to compute the TEC  
7 variations and compare the simulation results with TEC observations for the Tohoku-Oki EQ (Japan,  
8 11 March 2011, Mw 9.0). In the simulations, these authors assumed that the stress- associated  
9 current starts ~40 minutes before the EQ, and then linearly increases reaching its maximum  
10 magnitude at the time of the EQ main-shock. Comparisons with experimental values suggest that a  
11 dynamo current density of ~25 nA m<sup>-2</sup> is required to produce the observed variation of ~3 TECU.  
12

13 However, it must be noted that the relationship between ionospheric anomalies and electromagnetic  
14 signals generated by the EQ preparation is still controversial and highly debated, as demonstrated  
15 by the high number of papers reporting re-analysis of data and comments aiming to refute evidences  
16 of this correlation. For example, Masci et al. (2015) comment the findings of Heki (2011) and Heki  
17 and Enomoto (2013). After a re-analysis of the data, used by Heki (2011) to demonstrate the  
18 existence of a TEC anomaly 40 minutes before the EQs (2011 Tohoku-Oki and other M>8 EQs),  
19 Masci et al. (2015) conclude that this anomaly is due to an artefact introduced by the choice of the  
20 definition of the reference line adopted in analysing TEC variations.  
21  
22

### 23 *Pre-EQ ionospheric evidences from in-situ measurements*

24 Although many works on the possible pre-EQ effects in the ionosphere were also made with the  
25 early advent of satellites, it was with the DEMETER (Detection of Electro-Magnetic Emissions  
26 Transmitted from EQ Regions; 2004-2010) and CHAMP (CHallenging Minisatellite Payload;  
27 2000-2010) missions that most of the striking results were obtained.  
28

29 DEMETER was a French micro-satellite operated by CNES and specifically designed to the  
30 investigation of the Earth ionosphere disturbances due to seismic and volcanic activities. It operated  
31 for more than 6.5 years of scientific mission (2004-2010). The results from the analyses of this  
32 satellite dataset have statistically proved definitively the existence of the LAIC: what is still needed  
33 is to understand the deterministic details. Using the complete DEMETER data set (Píša et al. 2013),  
34 careful statistical studies were performed on the influence of seismic activity on the intensity of low

1 frequency EM waves in the ionosphere. In the satellite lifetime, several thousands of magnitude  
2 M5+ EQs occurred so constituting the seismic database. In particular the normalized probabilistic  
3 intensity obtained from the night-time electric field data is below the “normal” level, shortly (0 – 4  
4 hours) before the shallow (depth < 40 km) M5+ EQs at 1 – 2 kHz. Clear perturbations are observed  
5 a few hours before the EQs, as another example of “imminent” forecast: they are real, although they  
6 are weak and so far only statistically revealed. No similar effects were observed during the diurnal  
7 hours and for deeper EQs. It is interesting also to note that the spatial scale  $R$  of the affected area is  
8 approximately 350 km confirming relatively well the size of the EQ preparation zone estimated  
9 using the *Dobrovolsky et al. (1979)* formula. The main statistical decrease is observed at about 1.7  
10 kHz, corresponding approximately to the cut-off frequency of the first transverse magnetic (TM)  
11 mode of the Earth–ionosphere waveguide during the night-time. An increase of this cut-off  
12 frequency effect would therefore necessarily lead to the decrease of the power spectral density of  
13 electric field fluctuations observed by DEMETER in the appropriate frequency range, meaning a  
14 lower height of the ionosphere above the epicenter of the imminent EQ. As the EM waves  
15 propagating in the Earth-ionosphere wave-guide are mainly whistlers, this means that their  
16 propagation is disturbed above the epicenters of future EQs, instead of a change of their intensities.

17

18 Ryu et al. (2014a,b) took advantage of the simultaneous measurements of these two satellites: they  
19 analysed the electron density and temperature, ion density composition and temperature data from  
20 DEMETER ISL (Langmuir Probe), ICE (Electric Field Instrument) and IAP (Plasma Analyzer  
21 Instrument), together with CHAMP PLP data (electron density and temperature) and IONEX maps  
22 of  $vTEC$  (vertical TEC) from IGS (International GNSS Service). Their aim was the investigation of  
23 the ionospheric fluctuations related to the EQs occurred in September 2004 near to the south coast  
24 of Honshu, Japan (Ryu et al, 2014a) and Wenchuan EQ (M7.9) of 12 May 2008 (Ryu et al, 2014b).  
25 The main result was the detection of a gradual enhancement of the EIA (Equatorial Ionospheric  
26 Anomaly) intensity starting one month prior to the event, reaching its maximum eight days before,  
27 followed by a decreasing behavior, very likely due to an external electric field generated over the  
28 epicenter affecting the existing  $\mathbf{E} \times \mathbf{B}$  drifts responsible of the EIA.

29 By analysing the magnetic data from Swarm satellites of the European Space Agency, a recent  
30 paper (De Santis et al. 2017) finds some important patterns before the April 25, 2015 M7.8 Nepal  
31 EQ, that resemble the same obtained from the seismological analysis of the foreshocks.

32

33 *Pre-EQ atmospheric evidences*

1 The improvement and increase of satellite remote sensing missions go back to early 1980's. Since  
2 then, evidences of many types of infrared (IR) physics parameters have been recognized as useful to  
3 identify possible pre-EQ anomalies. Among them, the most cited are the Brightness Temperature  
4 (BT), Outgoing Longwave Radiation (OLR), Surface Latent Heat Flux (SLHF), Skin Surface  
5 Temperature (SST), and the atmospheric temperature at different altitudes. Although the topic is  
6 still debated or even controversial, many scientists agree that those parameters could change before  
7 EQs and so they are regularly recorded by satellite at regional and global scales. Examples of such  
8 variations of temperature or aerosols can be found in Pulinets et al. (2006), Jing et al. (2013), and  
9 Akhoondzadeh (2015). BT corresponds to the temperature of a black body that emits the same  
10 intensity as measured, and Xie and Ma (2015) found a clear BT anomaly in correspondence of  
11 Lushan M7 EQ (China). OLR is the emission of the terrestrial radiation from the top of the Earth's  
12 atmosphere to the space; it is controlled by the temperature of the earth and the atmosphere above it,  
13 in particular, by the water vapor and the clouds: as examples, Ouzounov et al. (2011) reported  
14 anomalies in this parameter days before the seismic events. SLHF describes the heat released by  
15 phase changes and shows an evident dependence on meteorological parameters such as surface  
16 temperature, relative humidity, wind speed, etcetera. SST is the temperature of the Earth's surface  
17 at radiative equilibrium (usually, the interface between soil and atmosphere, on lands; it is identical  
18 to Sea Surface Temperature over the seas), in contrast with the meteorological definition of surface  
19 temperature measured by air thermometers which take readings at approximately 1 meter above  
20 ground level. We will study the SST for the epicentral areas of the L'Aquila and Emilia main-  
21 shocks.

22  
23 The nature of the detected IR anomaly as a real temperature change, or perhaps just an emission in  
24 the IR frequency band, is a debated issue. In a recent paper, Piroddi et al. (2014) show a clear  
25 Thermal IR (TIR) anomaly preceding the 2009 M6.2 L'Aquila (Italy) EQ. The authors propose a  
26 mechanism of generation of electric currents in the lithospheric rocks when they are under stress  
27 and a consequent IR irradiation with no actual temperature change (e.g. Freund, 2011). However,  
28 some recent works identified SLHF (Qin et al., 2011) and surface temperature anomalies (Qin et al.,  
29 2012) occurring before large EQs, thus supporting the possibility for some actual change of  
30 temperature too. According to Freund (2018), this is only an apparent paradox because any  
31 stimulated IR emission from vibrationally very "hot" systems is not a "clean" process. Eventually,  
32 the system will "thermalize", meaning literally that each newly formed peroxy bond on the surface  
33 of the Earth will become a "hot spot", surrounded by a small halo where the neighboring atoms  
34 have actually increased their Joule temperature. Although the exact cause of such temperature raise

1 is still unknown, it is possible to definitely exclude the radon as a possible direct heat source, on the  
2 basis of the results of laboratory experiments conducted by Martinelli et al. (2015). Pulinets et al.  
3 (2015) resort to another role of radon as possible indirect source: it could drive particle ionization  
4 and aerosol aggregation, where the latent heat release can cause the found increase in the  
5 atmospheric temperature.

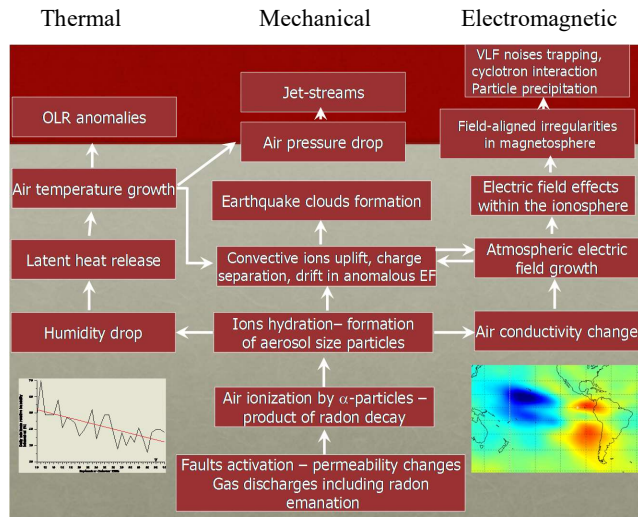
6  
7 Application of particular sophisticated techniques is mandatory to identify the anomalous signal in  
8 the TIR data. For instance, Tramutoli (2007, 2010), Aliano et al. (2008), and more recently Xiong et  
9 al. (2015) propose some robust satellite techniques that take into proper account the past behaviour  
10 of the signal under investigation: the typical seasonal and yearly background is computed and  
11 statistically significant deviation from it may represent the thermal anomaly. Recent interest was  
12 also addressed to air-quality data as possible indicators of an impending EQ (e.g. Hsu et al., 2010):  
13 these authors found a staggering increase in ambient SO<sub>2</sub> concentrations by more than one order of  
14 magnitude across Taiwan several hours prior to two (M6.8 and M7.2) significant EQs in the island.

15  
16 An interesting, although still controversial, emerging study concerns the EQ clouds (Guangmeng  
17 and Jie, 2013), suggesting that their formation is due to some local weather conditions caused by  
18 energy and particle exchanges between crust and atmosphere able to locally modify the global  
19 electric circuit during the EQ preparation phase (e.g. Harrison et al., 2014); or to create the  
20 conditions for electrical discharges in an atmosphere that may be the source of very high frequency  
21 (VHF) radio-emissions, sometime detected prior to large EQs (Ruzhin and Nomicos, 2007).  
22 Recently, the claim of unusual cloud formation prior strong EQs by Guangmeng and Jie (2013) was  
23 strongly questioned by Thomas et al. (2015) with a counter-analysis based on examination of 4  
24 years of satellite images and correlation analyses between linear-cloud formations and EQ  
25 occurrence.

### 26 27 *Physical Models*

28  
29 A plausible physical omni-comprehensive model justifying the great variety of evidences given  
30 before is the real difficult conundrum for the scientists in this field. There are many theories that  
31 attempt to describe the physical processes manifesting anomalous behaviour in some parameters  
32 before the occurrence of an EQ and try to explain what could cause these precursors. A review of  
33 these processes can be found in Pulinets and Boyarchuk (2004), Freund (2011), Pulinets and  
34 Ouzounov (2011) and the references therein (Figure 7).

1  
2



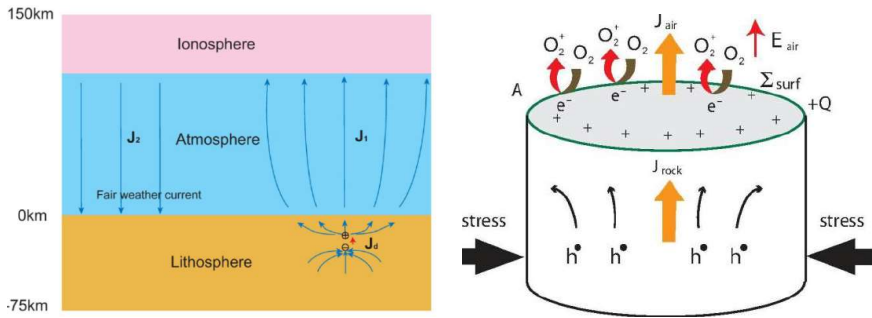
3  
4 **Fig.7.** Pulinets-Ouzonov LAIC model (adapted from Pulinets & Ouzonov, 2011; Pulinets et al., 2015)

5  
6 Among the many proposed mechanism of generations we can generally classify them as mechanical  
7 (atmospheric waves generated by earth motions) and electrical (electric fields in Earth's crust)  
8 sources: among the former, we can count the various kinds of atmospheric waves as internal or  
9 acoustic gravity waves (IGW and AGW, respectively), planetary waves and tides. In particular, the  
10 hypothesis of acoustic gravity waves generation before EQs was proposed by many authors (e.g.  
11 Pulinets and Boyarchuk, 2004).

12  
13 More complex and intriguing are the mechanisms that describe the anomalous electric field  
14 generation. A theory that can explain many observations is based on the emission of a radioactive  
15 gas or metallic ions before an EQ, which may change the distribution of electric potential above the  
16 surface of the Earth and then up to the ionosphere (e.g., Sorokin et al., 2001).

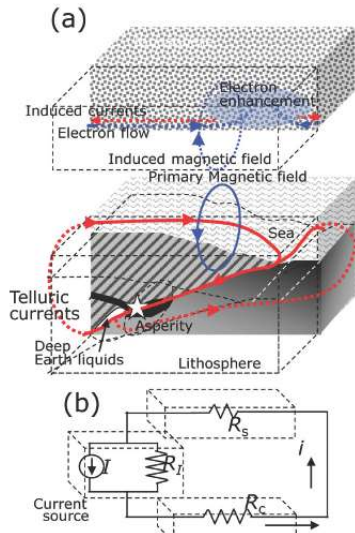
17  
18 Whatever its source is, penetration of the electric field into the ionosphere could induce anomalies  
19 in the ionospheric plasma density and/or conductivity, which are observed above seismic zones (see  
20 e.g., Liu et al., 2006; Kon et al., 2011). In contrast with this view, Harrison et al. (2010) proposed  
21 that radon emitted before an EQ would increase the conductivity of air at ground level and that the  
22 ensuing increase of current in the fair weather global circuit would lower the ionosphere. This  
23 mechanism is also supported by Pulinets et al. (2015). However, Freund et al. (2009) have

1 estimated that even if radon is coming out the ground in seismic areas, its contribution to the air  
 2 conductivity is of minor importance relative to the air ionization rate, which can be expected from  
 3 charge carriers from the rocks, the so-called positive-holes (or p-holes) (Figure 8).  
 4



5  
 6 **Fig. 8.** Freund model (adapted from Kuo et al., 2014)

7  
 8  
 9 They have shown experimentally that these mobile electric charge carriers flow out of the stressed  
 10 rocks (see Freund et al., 2009, and references therein) and, at the Earth's surface, they cause extra  
 11 ionization of the air molecules. However, the original experiments that detected these p-holes have  
 12 been recently contrasted (Dahlgren et al., 2014; but see also Scoville et al., 2015).



13  
 14 **Fig. 9.** Enomoto model (adapted from Enomoto, 2012)

1 Kuo et al. (2011, 2014) have shown that ionospheric density variations can be induced by changes  
2 of the current in the global electric circuit between the bottom of the ionosphere and the Earth's  
3 surface where electric charges associated with stressed rocks can appear. The interaction of the  
4 anomalous electric current with the geomagnetic field can even amplify the effect in the higher  
5 atmosphere (Kuo et al., 2014).

6 Enomoto (2012; Figure 9) has introduced a fault model that takes account of the couple interaction  
7 between EQ nucleation and deep Earth gases, and proposes a physical model of magnetic induction  
8 coupling with ionosphere before large offshore EQs.

9

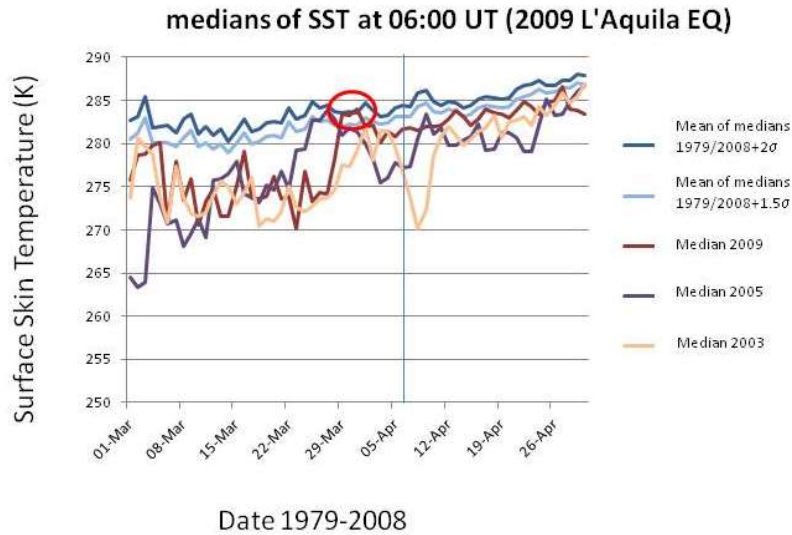
## 10 **11. Examples of thermal coupling before L'Aquila and Emilia EQs**

11

12 In the LAIC model, an important feature should be the coupling between lithosphere and low  
13 atmosphere (i.e. the troposphere) in terms of a thermal coupling. As said in the previous section, no  
14 general consensus exists about the fact that the thermal anomaly is just an infrared effect (e.g.  
15 Freund, 2011) or a real change of temperature (e.g. Qin et al., 2012). We do not want to express  
16 here a clear position in this debate. Rather, as didactical examples, we will show some SST studies  
17 for the same cases we analysed for the entropy, i.e. the 2009 L'Aquila and the 2012 Emilia  
18 sequences of EQs.

19

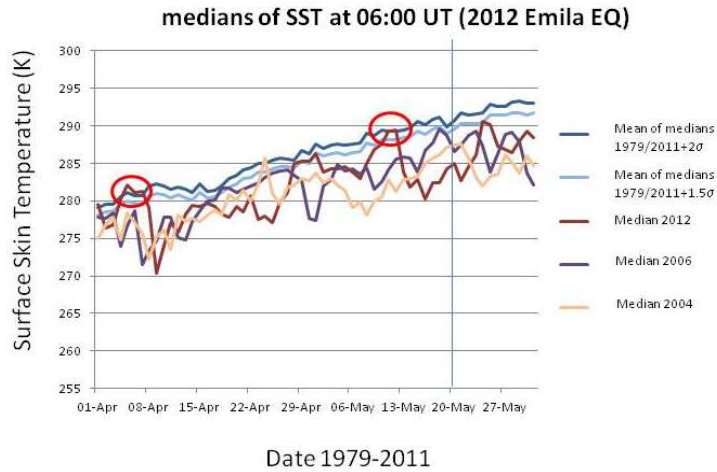
20 In each case study, we will consider the SST in the epicentral region about two months around the  
21 EQ occurrence, and then we will compare the temperatures with those measured in the same day, at  
22 the same time (06:00UT) in the time interval 1979-2008 (2011) for L'Aquila (Emilia) EQ. An  
23 anomaly of the physical quantity of concern is defined as a value that exceeds the mean (or median)  
24 by two times the standard deviation, and persists for at least two days (see also Piscini et al., 2017).



1  
 2 **Fig. 10.** Median behaviour of 2009 from 1 March to 30 April, compared with all 1979-2008 medians, and particular  
 3 comparison with 2003 and 2005 medians. All values have been estimated at the epicentre. The red oval indicates when  
 4 the thermal anomaly in 2009 is larger than or equal to 2 standard deviation,  $\sigma$  (as computed from the previous 1979-  
 5 2008 years) and persists for at least two days. The vertical line is the EQ occurrence.

6  
 7 Fig. 10 and Fig. 11 show the results for the two analyses. In detail, Fig.10 (Fig.11) shows for  
 8 L'Aquila (Emilia) EQ the median behaviour of 2009, from 1 March (April) to 30 April (31 May),  
 9 compared with all 1979-2008 (2011) medians, and particular comparison with 2003 (2004) and  
 10 2005 (2006) medians. For each day the use of the median was preferred because it was thought to  
 11 be a more robust indicator. The latter years have been used for comparison because no significant  
 12 seismicity occurred in those years in the two considered regions. All values have been estimated at  
 13 the EQ epicentre. The red oval indicates when the thermal anomaly in 2009 (2012) is larger than or  
 14 equal to 2 standard deviations,  $\sigma$  (as computed for each day from the previous 1979-2008 (2011)  
 15 years) and persists for at least two days. In both analyses, a clear anomaly is found around a week  
 16 before the EQ occurrence (vertical line in both figures). In the case of Emilia EQ, another persisting  
 17 anomaly is also found around 1 month and half before the main-shock.

18



1  
 2 **Fig. 11.** Median behaviour of 2012 from 1 April to 31 May, compared with all 1979-2011 medians, and particular  
 3 comparison with 2003 and 2005 medians. All values have been estimated at the epicentre. The red ovals indicate when  
 4 the thermal anomaly in 2012 is larger than or equal to 2 standard deviation,  $\sigma$  (as computed from the previous 1979-  
 5 2012 years) and persists for at least two days. The vertical line is the EQ occurrence.

6  
 7 These results confirm some previous studies on the possible thermal coupling in the two EQ cases  
 8 (e.g. Piroddi et al., 2014; Qin et al., 2012). The same Central Italy showed an analogous thermal  
 9 anomaly around 40 days before the recent 24 August 2016 M6 Amatrice EQ: Piscini et al. (2017)  
 10 applied the CAPRI algorithm (CAPRI stands for “Climatological Analysis for seismic PRecursor  
 11 Identification”) that removes the long-term trend over the whole day by day dataset. This procedure  
 12 is used mainly to remove a possible "global warming" effect, avoiding to classify as abnormal a  
 13 more recent year just because of global warming. These authors integrated the analysis of the skin  
 14 temperature also with total column water vapour and total column of ozone and made a confusion  
 15 matrix analysis for the last twenty years. As example, Table 2 shows the confusion matrix of the  
 16 validity of the skt as precursor applied to Central Italy earthquakes from 1994 to 2016. The  
 17 following results are obtained: overall accuracy= 74%, hit rate of success= 40%, false alarms=17%,  
 18 Cohen coefficient=0.23 (for more details on the corresponding definitions please see Piscini et al.  
 19 2017). These values confirm the validity of this thermal parameter as potential pre-earthquake  
 20 indication, at least for the area of concern, i.e. Central Italy.

21

skt	Seismicity	
	Yes	No

Yes	<u>2</u>	<u>3</u>
No	<u>3</u>	<u>15</u>

Table 2 Confusion matrix for pre/earthquake anomaly detection obtained from skt time series analysis since 1994 in Central Italy (adapted from Piscini et al., 2017).

Formattato: Normale, Interlinea: singola

Formattato: Tipo di carattere: Grassetto, Tutto maiuscole

Formattato: Normale, Interlinea: singola

## 12. Mutual Information and Transfer Information: a possible future direction

Geosystemics focuses on the inter-relations among the components composing the terrestrial complex system. For this reason, every statistical (or physical) quantity that measures these inter-relations is useful. However, given that the system under study is not usually linear, instead of linear quantities such as correlation coefficient or cross-correlation function between two variables belonging to linear processes, we have to resort to statistical quantities, which are more appropriate for nonlinear processes, as typical in a complex system.

Given two variables X and Y, characterising two processes of the phenomenon under study, we define the mutual information  $I(X, Y)$  extending definition (1) to two variables, i.e.:

$$I(X;Y) = \sum_{y \in Y} \sum_{x \in X} p(x,y) \cdot \log \left( \frac{p(x,y)}{p_1(x)p_2(y)} \right) \quad (10)$$

where  $p_1(x)$  and  $p_2(y)$  are the corresponding probabilities and  $p(x,y)$  is the joint probability.

However, this formulation does not provide hints about the direction of information transfer between process X and process Y, i.e. from a part of a system to another. For this purpose, it is possible to introduce a useful definition that quantifies the information flow in terms of the Kullback and Leibler entropy (Kullback and Leibler, 1951), which can be defined for a single process X as:

$$K_x = \sum_x p(x) \cdot \log[p(x)/q(x)] \quad (11)$$

The above quantity is the entropy related to the process X when a different probability  $q(x)$  is used instead of the true  $p(x)$ , and then adapt it in order to be applied to two variables taking into account of a proper delay in one (Schreiber 2000). The so-called transfer information (changing its sign it becomes the transfer entropy) provides also the direction of the information flow.

1 Here, we do not describe more details but we just want to emphasise the importance of quantifying  
2 direction of information flow amongst different parts or processes of the system under study,  
3 because often it is more important to know where the flow of information is going, instead of just  
4 estimating the information that is exchanged by the whole process between internal components or  
5 external ones (Ahlsvede et al. 2006).

6  
7 Applying this concept to two different time series can be useful to say if one is the master quantity  
8 (that represents the causal process) and the other the affected one. In all cases, where we would like  
9 to compare/correlate a seismic sequence with possible atmospheric or ionospheric series of  
10 precursors, the calculation of the transfer information would provide a robust answer.

### 14 **13. Conclusions**

15  
16 This paper has introduced the concepts of geosystemics, and then has shown its applications to  
17 some case studies. The spirit of geosystemics is to use some universal tools to look at some  
18 macroscopic quantities, such as the entropy, the Benioff strain, or the temperature to consequently  
19 deduce macroscopic properties of the physical system under study. An important frame is that of  
20 dynamical systems approaching a critical point, when the macroscopic properties of the system  
21 change dramatically. This could be the case of a sequence of EQs that culminates with a main-  
22 shock. Therefore, we showed some results obtained with the study of two recent Italian seismic  
23 sequences, the 2009 L'Aquila and the 2012 Emilia sequences.

24  
25 It is obvious that, being the study of EQs a very complex problem, the more characterizing  
26 parameters are analysed, the more robust the result will be. A recent and extensive example of this  
27 approach is given by Wu et al. (2016) for the case of the 2009 L'Aquila seismic sequence.

28  
29 A further question is how we can use the Big Data in geosciences and, in particular, to analyze  
30 precursory patterns of big earthquakes. Of course, the analysis of a greater number of data and the  
31 check of multiple models is perceptible that allows to find some type of pattern before an  
32 earthquake, that could be likely valid only for regions very localized. An extensive statistical big  
33 data analysis would be important to confirm or confute the individual case results (although no  
34 definitive conclusions can be arisen, because high correlation does not always mean causation;

1 however can be of great help in proposing a physical framework of the chain of processes that could  
2 occur before a large earthquake). An example of this approach is given by Piscini et al. (2017)  
3 where the validity of local climatological variations as possible seismic precursors in Central Italy  
4 has been statistically established.

5  
6 Finally, we hope that this investigation can contribute to the worldwide scientific debate and efforts  
7 in understanding the earthquake preparation phase in order to arm the scientific community and  
8 stakeholders against the natural disasters.

#### 14 **Acknowledgements**

15  
16 The authors thank ESA (European Space Agency) for funding the SAFE (Swarm for Earthquake  
17 study) project under STSE Swarm+Innovation Programme, and INGV (Istituto Nazionale di  
18 Geofisica e Vulcanologia) for funding LAIC-U (Lithosphere-Atmosphere-Ionosphere Coupling  
19 Understanding) and ECHO (Entropy and CHaOs: tools for studying and characterizing seismic  
20 sequences evolution) Projects, under which much work was undertaken for preparing this work.

1 **Appendix: Derivation of Eq. (6)**

2

3 The derivation of eq. (6) is as follows:

4

5 The probability density function corresponding to the Gutenberg-Richter law is

6 
$$p(M) = \frac{b \cdot 10^{-b(M-M_{\min})}}{\log e} \quad \text{with } M \geq M_{\min} \quad (\text{A1})$$

7

8 and, imposing  $M_{\min}=M_c$ , hence:

9 
$$H = - \int_{M_c}^{\infty} p(M) \cdot \log p(M) dM = - \int_{M_c}^{\infty} \frac{b \cdot 10^{-b(M-M_c)}}{\log e} \log \left( \frac{b \cdot 10^{-b(M-M_c)}}{\log e} \right) dM =$$

10 
$$= - \frac{b}{\log e} \int_{M_c}^{\infty} 10^{-b(M-M_c)} [\log b - b(M-M_c) - \log(\log e)] dM$$

11 
$$= - \frac{b}{\log e} \left\{ [\log b - \log(\log e)] \int_{M_c}^{\infty} 10^{-b(M-M_c)} dM - b \int_{M_c}^{\infty} (M-M_c) 10^{-b(M-M_c)} dM \right\}$$

12 
$$= - \frac{b}{\log e} \left\{ [\log b - \log(\log e)] \frac{\log e}{b} - b \frac{(\log e)^2}{b^2} \right\} = -\log b + \log(\log e) + \log e,$$

A(2)

13

14 which agrees with equation (6).

15

16

1 **References**

2

3 Ahlswede R., Baumer L., Cao N., Aydinian H., Blinovskiy V., Deppe C., Mashurian H. (Eds.),  
4 *General Theory of Information transfer and Combinatorics*, Springer-Verlag Berlin Heidelberg,  
5 2006.

6

7 Akhoondzadeh, M. , Ant Colony Optimization Detects Anomalous Aerosol Variations Associated  
8 with the Chile Earthquake of 27 February 2010. *Advances in Space Research* 55 (7). COSPAR:  
9 1754–63. doi:10.1016/j.asr.2015.01.016, 2015.

10

11 Aki, K. , Maximum likelihood estimate of  $b$  in the formula  $\log(N) = a - bM$  and its confidence limits,  
12 *Bull. Earthq. Res. Inst. Tokyo Univ.*, 43, 237–239, 1965.

13

14 Aki K. and Richards P, *Quantitative Seismology*, 2<sup>nd</sup> ed., Univ. Science Books, pp. 700, 2002.

15

16 Aliano, C., Corrado, R., Filizzola, C., Genzano, N., Pergola, N., and Tramutoli, V., Robust TIR  
17 Satellite Techniques for Monitoring Earthquake Active Regions: Limits, Main Achievements and  
18 Perspectives. *Annals of Geophysics* 51 (1): 303–17, 2008.

19

20 Baskoutas, I., Papadopoulos, G.A., Precursory Seismicity Pattern before Strong Earthquakes in  
21 Greece. *Research in Geophysics* 4 (1): 7–11. doi:10.4081/rg.2014.4899, 2014.

22

23 Beck, C., and Schlögl, F., *Thermodynamics of Chaotic Systems* (Cambridge University Press,  
24 Cambridge 1993) p. 306, 1993.

25

26 Bekenstein, J. D., Information in the Holographic Universe, *Scientific American*, 289, 2, August  
27 2003, p. 61, 2003.

28

29 Benioff, H., Seismic evidence for the fault origin of oceanic deeps, *Geol. Soc. Am. Bull.*, 60, 1837-  
30 1856, 1949.

31

32 Bizzarri A., On the deterministic description of earthquakes, *Review of Geophysics*, 49, 1-32, 2011.

33

1 Bizzarri A., Rupture speed and slip velocity: what can we learn from simulated earthquakes?, *Earth*  
2 *Planet. Sci. Lett.*, 317-318, 196-203, 2012.

3

4 Bizzarri A., The mechanics of seismic faulting: Recent advances and open issues, *La Rivista del*  
5 *Nuovo Cimento*, 4, 37, 181-271, 2014.

6

7 Bowman, D.D., Ouillon, G., Sammis, C.G., Sornette, A., Sornette, D., An observational test of the  
8 critical earthquake concept. *J. Geophys. Res.* 103, 24,359–24,372, 1998.

9

10 Bunde, A., Kropp, J., and Schellnhuber, H. J., *The Science of Disasters*. Climate disruptions, heart  
11 attacks, and market crashes, Springer Berlin, 2002.

12

13 Bufe, C.G., Varnes, D.J. , Predictive modelling of the seismic cycle of the greater San Francisco  
14 Bay region, *J. Geoph. Res.*, 98, B6, 9871-9883, 1993.

15

16 Butz, S. D., *Science of Earth Systems*. Thomson Learning, 2004.

17

18 Chuvieco E. and Huete A., *Fundamentals of satellite remote sensing*, CRC Press, pp. 448, 2009.

19

20 Cicerone, R.D., Ebel, J.E., Britton, J. , A Systematic Compilation of Earthquake Precursors.  
21 *Tectonophysics* 476 (3-4). Elsevier B.V.: 371–96. doi:10.1016/j.tecto.2009.06.008, 2009.

22

23 Contadakis, M., Arabelos, D., Vergos, G., Spatalas, S., TEC Variations over Mediteranean before  
24 and during the Strong Earthquake (  $M = 6.2$  ) of 12th October 2013 in Crete, Greece. *Phys. & Chem.*  
25 *Earth*, 16 (April 2009). Elsevier Ltd: 2319. doi:10.1016/j.pce.2015.03.010, 2014.

26

27 Dabas, R.S., Das, R.M., Sharma, K., Pillai, K.G.M., Ionospheric precursors observed over low  
28 latitudes during some of the recent major earthquakes, *J. Atmos. Solar-Terr. Phys.*, 69, 1813- 1824,  
29 2007.

1

2 Dahlgren, P.R., Johnston, M.J.S., Vanderbilt, V.C. and Nakaba, R.N., Comparison of the stress-  
3 stimulated current of dry and fluid saturated gabbro samples. *Bull. Seismol. Soc. Am.* 104, 2662–  
4 2672, 2014.

5

6 De Santis A., Geosystemics, *Proceedings 3<sup>rd</sup> IASME/WSEAS International Conference on Geology  
7 and Seismology (GES'09)*, Cambridge, 36-40, 2009.

8

9 De Santis A., Geosystemics, entropy and criticality of earthquakes: a vision of our planet and a key  
10 of access, in *Nonlinear phenomena in Complex Systems: from Nano to Macro Scale*, ed. E. Stanley  
11 and D. Matrasulov, NATO Science for Peace and Security Series – C: Environmental Security, 3-20,  
12 2014.

13

14 De Santis A., Qamili E., Geosystemics: a systemic view of the Earth's magnetic field and  
15 possibilities for an imminent geomagnetic transition, *Pageoph*, 172, 75-89, 2015.

16

17 De Santis A., Cianchini G., Favali P., Beranzoli L., Boschi E., The Gutenberg–Richter Law and  
18 Entropy of Earthquakes: Two Case Studies in Central Italy, *Bull. Seismol. Soc. Am.*, Vol. 101, No. 3,  
19 1386–1395, 2011a.

20

21 De Santis A., Qamili E. and Cianchini G., Ergodicity of the recent geomagnetic field, *Physics of  
22 the Earth and Planetary Interiors*, 186, 103–110, 2011b.

23

24 De Santis, A., Cianchini, G., Di Giovambattista, R., Accelerating moment release revisited:  
25 Examples of application to Italian seismic sequences, *Tectonophysics*, Volume 639, 12 January  
26 2015, pag. 82-98, 2015a.

27

28 De Santis et al., Geospace perturbations induced by the Earth: the state of the art and future trends,  
29 *Phys. & Chem. Earth*, 85-86, 17-33, 2015b.

30

31 De Santis A. et al., Potential earthquake precursory pattern from space: the 2015 Nepal event as  
32 seen by magnetic Swarm satellites, *Earth and Planetary Science Letters*, 461, 119-126, 2017.

33

1 Grandy, W.T., Jr, *Entropy and the Time Evolution of Macroscopic Systems*, Oxford University  
2 Press, Oxford, 2008.

3

4 Gutenberg, B., and C. F. Richter, Frequency of earthquakes in California, *Bull. Seismol. Soc. Am.*,  
5 34, 185–188, 1944.

6

7 Dieterich, J.H., A constitutive law for rate of earthquake production and its application to  
8 earthquake clustering, *J. Geophys. Res.* 99, 2601-2618, 1994.

9

10 Dobrovolski, I.P., Zubkov, S.I. & Miachin, V.I., Estimation of the size of Earthquake preparation  
11 zones, *Pure appl. Geophys.*, vol. 117, 1025- 1044, 1979.

12

13 Dobrovolski, I.P., N.I. Gershenzon, M.B. Gokhberg, Theory of electrokinetic effects occurring at  
14 the final stage in the preparation of a tectonic earthquake, *Phys. Earth Planet. Inter.*, 57, 1-2, 144-  
15 156, 1989.

16

17 Enomoto, Y. , Coupled interaction of earthquake nucleation with deep Earth gases: a possible  
18 mechanism for seismo-electromagnetic phenomena. *Geophys. J. Inter.* 191, 1210–1214, 2012.

19

20 Favali P., Beranzoli L. and De Santis A. , *Seafloor Observatories: A new vision of the Earth from*  
21 *the Abyss*, Springer - Praxis Publishing, 1-2, 2015.

22

23 Freund, F.T., Pre-earthquake signals: underlying physical processes. *J. Asian Earth Sci.* 41, 383–  
24 400, 2011.

25

26

27 Freund, F.T., Interactive comment, Solid Earth Discuss., <https://doi.org/10.5194/se-2017-120-SC1>,  
28 2018,

29

30 Freund, F.T., Kulahci, I.G., Cyr, G., Ling, J., Winnick, M., Tregloan-Reed, J., Freund, M.M. , Air  
31 ionization at rock surfaces and pre-earthquake signals. *J. Atmos. Sol. Terr. Phys.* 71 (17–18), 1824–  
32 1834. <http://dx.doi.org/10.1016/j.jastp.2009.07.013>, 2009.

**Formattato:** Tipo di carattere: Non Grassetto, Inglese (Stati Uniti)

**Formattato:** Inglese (Stati Uniti)

**Formattato:** Inglese (Stati Uniti)

1  
2 Gabrielov et al., Critical transitions in colliding cascades, *Phys. Rev. E*, 62, N.1, 237-249, 2000.  
3  
4 Guangmeng, G., Jie, Y. , Three attempts of earthquake prediction with satellite cloud images. *Nat.*  
5 *Hazards Earth Syst. Sci.* 13, 91–95, 2013.  
6  
7 Hardebeck, J.L., Felzer, K.R., Michael, A.J., Improved test results reveal that the accelerating  
8 moment release hypothesis is statistically insignificant, *J. Geophys. Res.*, 113, B08310, 2008.  
9  
10 Harrison, R.G., Aplin, K.L., Rycroft, M.J., Atmospheric electricity coupling between earthquake  
11 regions and the ionosphere. *J. Atmos. Sol. Terr. Phys.* 72, 376–381, 2010.  
12  
13 Harrison, R.G., Aplin, K.L., Rycroft, M.J., Earthquake-cloud coupling through the global  
14 atmospheric electric circuit. *Nat. Hazards Earth Syst. Sci.* 14, 773– 777, 2014.  
15  
16 Heki, K., Ionospheric Electron Enhancement Preceding the 2011 Tohoku-Oki Earthquake.  
17 *Geophysical Research Letters* 38 (17): 1–5. doi:10.1029/2011GL047908, 2011.  
18  
19 Heki, K., Enomoto, Y. Preseismic Ionospheric Electron Enhancements Revisited. *Journal of*  
20 *Geophysical Research: Space Physics* 118 (10): 6618–26. doi:10.1002/jgra.50578, 2013.  
21  
22 Hobara, Y., Parrot, M., Ionospheric perturbations linked to a very powerful seismic event, *J. Atmos.*  
23 *Solar-Terr. Phys.*, 67, 677–685, doi:10.1016/j.jastp.2005.02.006, 2005.  
24  
25 Holliday, J.R., Chen, C.-C., Tiampo, K.F., Rundle, J.B., Turcotte, D.L., Donnellan, A., A RELM  
26 earthquake forecast based on pattern informatics. *Seismol. Res. Lett.*, 78, 87–93, 2007.  
27  
28 Hough, S., *Predicting the Unpredictable: The Tumultuous Science of Earthquake Prediction.*  
29 Princeton University Press, 2009.  
30  
31 Hsu, S.C., Huang, Y.T., Tu, J.Y., Huang, Jr-Chung, Engling, G., Lin, C.Y., Lin, F.J., Huang, C.H.,  
32 Evaluating real-time air-quality data as earthquake indicator. *Sci. Total Environ.* 408, 2299-2304,  
33 2010.  
34

1 Ihara, S. , *Information Theory for Continuous Systems*, World Scientific, London, 1993.  
2  
3 Jacobson, M. , R. J. Charlson, H. Rodhe and G. H. Orians (Eds.) *Earth System Science, From*  
4 *Biogeochemical Cycles to Global Changes* (2nd ed.). London: Elsevier Academic Press, 2000.  
5  
6 Jing, F., Shen, X.H., Kang, C.L., Xiong, P., Variations of multi-parameter observations in  
7 atmosphere related to earthquake. *Nat. Hazards Earth Syst. Sci.* 13, 27-33, 2013.  
8  
9 Kanamori H., The nature of seismicity patterns before large earthquakes, in *Earthquake Prediction*  
10 (Simpson D.W and Richards P.G. ed.s), American Geophysical Union, Washington, D.C., doi:  
11 10.1029/ME004p001, 1981.  
12  
13 Keilis-Borok, V.I., Kossobokov, V.G., Premonitory activation of earthquake flow: Algorithm M8,  
14 *Phys. Earth. Planet. Inter.*, 61, 73-83, 1990.  
15  
16 Kelley M.C., *The earth's ionosphere. Plasma physics and electrodynamics.* 2<sup>nd</sup> Edition, Elsevier,  
17 Amsterdam, 2009.  
18  
19 Klir G.J, *Uncertainty and Information. Foundations of Generalized Information Theory.* J Wiley &  
20 Sons, Inc, Hoboken, New Jersey, pp.499, 2006.  
21  
22 Kon, S., Nishihashi, M., Hattori, K., Ionospheric anomalies possibly associated with M<sub>6.0</sub>  
23 earthquakes in the Japan area during 1998–2010: case studies and statistical study. *J. Asian Earth*  
24 *Sci.* 41, 410–420, 2011.  
25  
26 Kossobokov, V.G. , Earthquake prediction: 20 years of global experiment, *Nat. Hazards*, 69, 1155-  
27 1177, 2013.  
28  
29 Kullback, S., Leibler, R.A., On information and sufficiency. *The Annals of Mathematical Statistics*  
30 22 (1), 79–86,1951.  
31

1 Kuo, C.L., Huba, J.D., Joyce, G., Lee, L., Ionosphere plasma bubbles and density variations  
2 induced by pre-earthquake rock currents and associated surface charges. *J. Geophys. Res.* 116,  
3 A10317. <http://dx.doi.org/10.1029/2011JA016628>, 2011.  
4  
5 Kuo, C.L., Lee, L., Huba, J.D., An improved coupling model for the lithosphere– atmosphere–  
6 ionosphere system. *J. Geophys. Res.* <http://dx.doi.org/10.1002/2013JA019392>, 2014.  
7  
8 Kuo, C. L., L. C. Lee, and K. Heki, Preseismic TEC changes for Tohoku-Oki earthquake:  
9 Comparisons between simulations and observations. *Terr. Atmos. Ocean. Sci.*, 26, 63-72, doi:  
10 10.3319/TAO.2014.08.19.06(GRT), 2015.  
11  
12 Jin, S., Occhipinti, G., Jin, R., GNSS Ionospheric Seismology: Recent Observation Evidences and  
13 Characteristics. *Earth-Science Reviews* 147. Elsevier B.V.: 54–64.  
14 doi:10.1016/j.earscirev.2015.05.003, 2015.  
15  
16 Liu, J.Y., Chen, Y.I., Chuo, Y.J., Chen, C.S., A statistical investigation of pre- earthquake  
17 ionospheric anomaly. *J. Geophys. Res.* 111, A05304. [http:// dx.doi.org/10.1029/2005JA011333](http://dx.doi.org/10.1029/2005JA011333),  
18 2006.  
19  
20 Lovelock J. E., Gaia as seen through the atmosphere, *Atmospheric Environment* 6 (8): 579–580.  
21 1972.  
22  
23 Mancini, F., Galeandro, A., De Giglio, M., Barbarella, M., Assessing Ionospheric Activity by Long  
24 Time Series of GNSS Signals: The Search of Possible Connection with Seismicity. *Physics and*  
25 *Chemistry of The Earth* 16. Elsevier Ltd: 12002. doi:10.1016/j.pce.2014.10.005, 2014.  
26  
27 Martinelli, G., Solecki, A.T., Tchorz-Trzeciakiewicz, D.E., Piekarz, M., Grudzinska, K.K.,  
28 Laboratory Measurements on Radon Exposure Effects on Local Environmental Temperature:  
29 Implications for Satellite TIR Measurements. *Physics and Chemistry of the Earth, Parts A/B/C*,  
30 April. doi:10.1016/j.pce.2015.03.007, 2015.  
31  
32 Masci, F, Thomas, J.N., Villani, F., Secan, JA., Rivera, N., On the Onset of Ionospheric Precursors  
33 40 Min before Strong Earthquakes. *Journal of Geophysical Research: Space Physics*.  
34 doi:10.1002/2014JA020822, 2015.

1  
2  
3  
4  
5  
6  
7  
8  
9  
10  
11  
12  
13  
14  
15  
16  
17  
18  
19  
20  
21  
22  
23  
24  
25  
26  
27  
28  
29  
30  
31  
32

Meyers R. A., *Extreme environmental events*. Springer, New York, p 1250, 2009.

Mignan A., The Stress Accumulation Model: Accelerating Moment Release and Seismic Hazard, *Adv. In Geophysics*, 49, 67–201, 2008.

[Molchan G. and L. Romashkova, Gambling score in earthquake prediction analysis, Geoph. J. Int., 184, 1445–1454, 2011.](#)

Formattato: Giustificato, Interlinea: 1.5 righe

Nanjo K.Z., Rundle, J.B., Holliday. J.R., Turcotte, D.L., Pattern Informatics and its application for optimal forecasting of large earthquakes in Japan, *Pure app. Geophys.*, 163, 2417-2432, 2005.

Nott J., *Extreme events: a physical reconstruction and risk assessment*. Cambridge University Press, Cambridge, p 297, 2006.

Ondoh, T., Anomalous sporadic-E layers observed before M 7.2 Hyogo-ken Nanbu earthquake; Terrestrial gas emanation model, *Adv. Polar Upper Atmos. Res.*, 17, 96-108, 2003.

Ondoh, T., Hayakawa, M., Synthetic study of precursory phenomena of the M7.2 Hyogo-ken Nanbu earthquake, *Phys. Chem. Earth*, 31, 378-388, 2006.

Ouzounov, D., Pulinets, S., Hattori, K., Kafatos, M., Taylor., P., Atmospheric Signals Associated with Major Earthquakes. *A Multi-Sensor Approach*, Chapter 9, no. March: 1–23. <http://hdl.handle.net/2060/20110012856>, 2011.

Codice campo modificato

Peduzzi P., Is climate change increasing the frequency of hazardous events?, *Environment & Poverty Times*, n.3, 7, 2005.

Perrone, L., Korsunova, L., Mikhailov, A., Ionospheric precursors for crustal earthquakes in Italy, *Ann. Geophysicae*, 28, 941-950, 2010.

1 Piša, D., F. Němec, O. Santolik, M. Parrot, and M. Rycroft, Additional attenuation of natural VLF  
2 electromagnetic waves observed by the DEMETER spacecraft resulting from preseismic activity, *J.*  
3 *Geophys. Res. Space Physics*, 118, doi:10.1002/jgra.50469, 2013.  
4  
5 Piscini A., De Santis A., Marchetti D. and Cianchini G., A multi-parametric climatological  
6 approach to study the 2016 Amatrice-Norcia (Central Italy) earthquake preparatory phase, *Pure*  
7 *appl. Geophys.*, in press, 2017.  
8  
9 Piroddi, L., Ranieri, G., Freund, F., Trogu, A., Geology, Tectonics and Topography Underlined by  
10 L'Aquila Earthquake TIR Precursors. *Geophysical Journal International* 197 (3): 1532–36.  
11 doi:10.1093/gji/ggu123, 2014.  
12  
13 Pulinets, S.A., Boyarchuk, K.A., *Ionospheric Precursors of Earthquakes*. Springer Verlag, 2004.  
14  
15 Pulinets, S.A., Ouzounov, D., Ciraolo, L., Singh, R., Cervone, G., Leyva, A., Dunajceka, M.,  
16 Karelin, A.V., Boyarchuk, K.A., Kotsarenko, A., Thermal, atmospheric and ionospheric anomalies  
17 around the time of the Colima M7.8 earthquake of 21 January 2003. *Annales Geophysicae*,  
18 European Geosciences Union (EGU), 24 (3), pp.835-849, 2006.  
19  
20 Pulinets, S.A., Ouzounov, D., Lithosphere–Atmosphere–Ionosphere Coupling (LAIC) model. An  
21 unified concept for earthquake precursors validation. *J. Asian Earth Sci.* 41, 371-382, 2011.  
22  
23 Pulinets S.A., Ouzounov D.P., Karelin A.V., Davidenko D.V., Physical bases of the generation of  
24 short-term earthquake precursors: a complex model of ionization-induced geophysical processes in  
25 the Lithosphere-Atmosphere-Ionosphere-Magnetosphere System, *Geomagnetism & Aeronomy*, No.4,  
26 522-539, 2015.  
27  
28 Qin, K., Wu, L.X., De Santis, A., Wang, H., Surface latent heat flux anomalies before the Ms 7.1  
29 New Zealand earthquake 2010. *Chinese Sci. Bull.* 56 (31), 3273–3280, 2011.  
30  
31 Qin, K., Wu, L.X., De Santis, A., Cianchini, G., Preliminary analysis of surface temperature  
32 anomalies that preceded the two major Emilia 2012 earthquakes (Italy). *Ann. Geophys.* 55 (4), 823–  
33 828, 2012.  
34

1 Rundle, J.B., Tiampo, K.F., Klein, W., Martins, J.S.S., Self-organization in leaky threshold  
2 systems: The influence of near mean field dynamics and its implications for earthquakes,  
3 neurobiology and forecasting, *Proc. Natl. Acad. Sci. U.S.A.*, 99, suppl. 1,2514-2521, 2002.  
4  
5 Row, R.V., Acoustic-gravity waves in the upper atmosphere due to a nuclear detonation and an  
6 earthquake. *J. Geoph. Res.* 72 (5), 1599–1610, 1967.  
7  
8 Ruzhin, Y., Nomicos, C. , Radio VHF precursors of earthquakes. *Nat. Hazard* 40, 573–583, 2007.  
9  
10 Schneider, S. and Boston P., *The Gaia Hypothesis and Earth System Science*. University of Florida.  
11 MIT Press, 1992.  
12  
13 Scholz C.H., The frequency-magnitude relation of microfracturing in rock and its relation to  
14 earthquakes, *Bull. seismol. Soc. Am.*, 58, 399-415, 1968.  
15  
16 Scholz, C.H., *The Mechanics of Earthquake and Faulting*, vol. xxiv. Cambridge Univ. Press,  
17 Cambridge/New York (471 pp.), 2002.  
18  
19 Schorlemmer, D., S. Wiemer, and M. Wyss, Variations in earthquake size distribution across  
20 different stress regimes, *Nature*, 437, 539–542, 2005.  
21  
22 Schreiber, T. , Measuring Information Transfer, *Phys. Rev. Lett.*, 85, 2, 461-464, 2000.  
23  
24 Shebalin P., Keilis-Borok, V., Gabrielov A., Zaliapin I., Turcotte D., Short-term earthquake  
25 prediction by reverse analysis of lithosphere dynamics, *Tectonophysics*, 413, 63 – 75, 2006.  
26  
27 Scoville, J., Heraud, J., Freund, F., Pre-Earthquake Magnetic Pulses. *Nat.Hazards Earth Scyst. Sci.*,  
28 15, 1873-1880, 2015.  
29  
30 Shannon, C. E., A mathematical theory of communication, *Bell Syst.Tech. J.* 27, 379, 623, 1948.  
31  
32 Signanini P., De Santis A., Power-law frequency distribution of *H/V* spectral ratio of seismic  
33 signals: evidence for a critical crust, *Earth Planets Space*,64, 49-54, 2012.  
34

- 1 Silina, A.S., Liperovskaya, E.V., Liperovsky, V.A., Meister, C.V. Ionospheric phenomena before  
2 strong earthquakes, *Natural Hazards and Earth System Sciences*, 1, 113-118, 2001.
- 3
- 4 Skinner BJ, Porter SC., *The blue planet: an introduction to earth system science*. Wiley VCH, New  
5 York, 1995.
- 6
- 7 Sobolev G.A., Huang Q. and Nagao T., Phases of earthquake's preparation and by chance test of  
8 seismic quiescence anomaly, *J. Geodynamics*, 33, 4-5, 413-424, 2002.
- 9
- 10 Sorokin, V.M., Chmyrev, V.M., Yaschenko, A.K.-, Electrodynamic model of the lower atmosphere  
11 and the ionosphere coupling. *J. Atmos. Sol. Terr. Phys.* 63, 1681–1691, 2001.
- 12
- 13 Stanley, H. E., *Introduction to phase transitions and critical phenomena*. Oxford University  
14 Press, New York, 1971
- 15
- 16 [Sugan, M., A. Kato, H. Miyake, S. Nakagawa, and A. Vuan, The preparatory phase of the 2009 Mw  
17 6.3 L'Aquila earthquake by improving the detection capability of low-magnitude foreshocks,  
18 \*Geophys. Res. Lett.\*, 41, 6137–6144, doi:10.1002/2014GL061199, 2014.](#)
- 19
- 20 Takens F., Detecting strange attractors in turbulence, Proceedings “*Dynamical Systems and  
21 Turbulence, Warwick 1980*”, Lecture Notes in Mathematics, Volume 898. ISBN 978-3-540-11171-  
22 9. Springer-Verlag, 1981.
- 23
- 24 Thomas, J.N., Masci, F., and Love, J.J. , On a report that the 2012 M 6.0 earthquake in Italy was  
25 predicted after seeing an unusual cloud formation, *Nat. Hazards Earth Syst. Sci.*, 15, 1061-1068,  
26 doi:10.5194/nhess-15-1061-2015, 2015.
- 27
- 28 Tiampo, K. F., Rundle, J. B., Klein, W., Premonitory seismicity changes prior to the Parkfield and  
29 Coalinga earthquakes in southern California, *Tectonophysics*, 413, 77–86, 2006.
- 30
- 31 Tramutoli, V., Robust satellite techniques (RST) for natural and environmental hazards monitoring  
32 and mitigation: theory and applications. In: *Proceedings 2007 International Workshop on the  
33 Analysis of Multi-temporal Remote Sensing Images*,  
34 <http://dx.doi.org/10.1109/MULTITEMP.2007.4293057>, 2007.

Codice campo modificato

1  
2 Tramutoli, V. , Using RST approach and EOS-MODIS radiances for monitoring seismically active  
3 regions: a study on the 6 April 2009 Abruzzo earthquake. *Nat. Hazards Earth Syst. Sci.* 10, 239–  
4 249, 2010.  
5  
6 Tyupkin, Y. S., Di Giovambattista, R. , Correlation length as an indicator of critical point behavior  
7 prior to a large earthquake, *Earth Planet. Sci. Lett.*, 230, 85 – 96, doi:10.1016/j.epsl.2004.10.037,  
8 2005.  
9  
10 Ulam S. M. and von Neumann J., On the Combinations of Stochastic and Deterministic Processes,  
11 *Bull. Amer. Math. Soc.* 53, 1120, 1947.  
12  
13 Utsu, T., Estimation of parameter values in the formula for the magnitude-frequency relation of  
14 earthquake occurrence, *Zisin* 31, 367-382, 1978.  
15  
16 Wang, L.-W., Shen, X.-H., Zhang, Y., Yan,R., Preliminary proposal of scientific data verification in  
17 CSES mission. *Earthquake Science* 28 (4): 303–310. doi: dx.doi.org/10.1007/s11589-015-0131-2,  
18 2015.  
19  
20 Wu L.X., Zheng S., De Santis A., Qin K., Di Mauro R., Liu S.J. and Rainone M. L., Geosphere  
21 Coupling and Hydrothermal Anomalies before the 2009 Mw 6.3 2 L’Aquila Earthquake in Italy,  
22 *Nat. Hazards Earth Syst. Sci.*, 16, 1859-1880, doi:10.5194/nhess-2015-346, 2016.  
23  
24 Xie, T. and Weiyu, M., Possible Thermal Brightness Temperature Anomalies Associated with the  
25 Lushan (China) MS7.0 Earthquake on 20 April 2013. *Earthquake Science* 28 (1): 37–47.  
26 doi:10.1007/s11589-014-0106-8, 2015.  
27  
28 Xiong, Pan, Xuhui Shen, Xingfa Gu, Qingyan Meng, Yaxin Bi, Liming Zhao, Yanhua Zhao, Yan Li,  
29 and Jianting Dong, Satellite Detection of IR Precursors Using Bi-Angular Advanced along-Track  
30 Scanning Radiometer Data: A Case Study of Yushu Earthquake. *Earthquake Science* 28 (1): 25–36.  
31 doi:10.1007/s11589-015-0111-6, 2015.  
32

1 Xu, T., Hu, Y.L., Wang, F.F., Chen Z., Wu J., Is there any difference in local time variation in  
2 ionospheric F2 layer disturbances between earthquake induced and Q- disturbances events?, *Ann.*  
3 *Geophysicae*, 33, 687-695, 2015.

4 [Zechar, J.D. & Zhuang, J., Risk and return: evaluating RTP earthquake predictions, \*Geophys. J. Int.\*,  
5 \*182\*, 1319–1326. 2010.](#)

6  
7 Zoller, G., Hainzl, S. A systematic spatiotemporal test of the critical point hypothesis for large  
8 earthquakes. *Geophys. Res. Lett.*, 29, 1558, 2002.

9  
10

**Formattato:** Inglese (Stati Uniti)

**Formattato:** Giustificato, Interlinea: 1.5 righe